MOLECULAR CHARACTERIZATION OF TWO HUMAN LENS EPITHELIAL CELL LINES: HLE-B3 AND SRA01/O4

by

Joshua R. Barton

A thesis submitted to the Faculty of the University of Delaware in partial fulfillment of the requirements for the degree of Honors Degree in Major with Distinction

Spring 2016

© 2016 Joshua R. Barton
All Rights Reserved

MOLECULAR CHARACTERIZATION

OF TWO HUMAN LENS EPITHELIAL

CELL LINES: HLE-B3 AND SRA01/O4

by

Joshua R. Barton

Approved: _____

Salil Lachke, PhD
Professor in charge of thesis on behalf of the Advisory Committee

Approved: _____

Melinda Duncan, PhD
Committee member from the Department of Biological Sciences

Approved: _____

John Jungk, PhD
Committee member from the Board of Senior Thesis Readers

Approved: _____

Michael Arnold, Ph.D.
Directory, University Honors Program

ACKNOWLEDGMENTS

TABLE OF CONTENTS

LIST OF TABLES vi
LIST OF FIGURES vii
ABSTRACT ix

1 INTRODUCTION 1

1.1 The Mammalian Optic Lens 1
1.2 Cataract: The World's Leading Cause of Blindness 4
1.3 Predicting Cataract-Associated Genes 7

1.4 RNA Granules and Cataract 9
1.5 UV, the Lens, and RNA granules 16
1.6 Cell Lines and In Vitro Models for the Human Optic Lens 18

2 MATERIALS AND METHODS 24

2.1 Cell Culture 24
2.2 Authentication of Cell Lines 24
2.3 Whole-genome dataset Analyses 26
2.4 RT-PCR and qRT-PCR Analysis 26
2.5 Immunostaining Analysis 28
2.6 Stress Conditions 30
2.7 Quantification of RNA Granules 31

3 RESULTS 32

3.1 Human LECs Authenticated as Human-Derived cells 32
3.2 Human LECs Show Gene Expression Profiles Similar to *In Vivo* Lenses and *In Vitro* Validated Models 33
3.3 RT-PCR Validates Human LECs Expression of Key Lens Enriched Genes 36
3.4 Chemical Stress Significantly Induces Stress Granules and Processing Bodies in Human LECs 37
3.5 UV Stress Significantly Induces Stress Granules and Processing Bodies in Mouse and Human LECs 40

4 DISCUSSION 46

REFERENCES 52

A SUPPLEMENTARY METHODS 65

LIST OF TABLES

Table 2.2: Primer sequences used for STR analysis..... 25

LIST OF FIGURES

Figure 1.1.1: Organization of the lens. 3

Figure 1.2.1: The lens functions to focus light on to the retina 5

Figure 1.2.2: Incidence of Cataract in the United States 6

Figure 1.3.1 Identification by *iSyTE* of *Celf1* as a highly len-enriched gene 9

Figure 1.4.1: Conserved function of Tdrd7 in vertebrate lens development 10

Figure 1.4.2: Processing bodies and Stress granules 15

Figure 1.5.1: The penetration light through the eye as a function of wavelength. 17

Figure 1.5.2: HeLa Cells stressed with UVC exhibit stress granules hours after irradiation 18

Figure 1.6.1: Graphic of the total publications of both human LEC lines 22

Figure 1.6.2 The human lens epithelial cell lines SRA01/04 and HLE-B3 22

Figure 1.6.3: Fluorescence micrographs of cells treated with mouse anti-SV40 antibodies 23

Figure 3.1.1: STR analysis of the human lens epithelial cell lines HLE-B3 and SRA01/04. 33

Figure 3.2.1: Comparative analysis of gene expression profiling between lens and lens epithelial cell lines 34

Figure 3.2.2: Comparative microarray analysis of select lens expressed genes in human and mouse lens epithelial cell lines. 35

Figure 3.3.1: Investigation of select lens-expressed genes in human lens epithelial cell lines 37

Figure 3.4.1: RNA granule formation in human lens cell lines 39

Figure 3.4.2: RNA granules response of human lens cell lines to chemical stress 40

Figure 3.5.1: UV-induced RNA granules in mouse lens epithelial cell line 21EM15 . 41

Figure 3.5.2: Dosage effect of UV-induced stress on 21EM15 cells 43

Figure 3.5.3 Response of human lens epithelial cell lines to UV stress..... 44

Figure 3.5.4: Recovery time-course of SRA01/04 after UV stress 45

ABSTRACT

The ocular lens is a transparent tissue that focuses light on the retina, allowing high-resolution vision. The loss of lens transparency causes an eye defect termed cataract, which is the leading cause of blindness worldwide. Half of the U.S. population above age 80 is affected by cataracts, for which surgical treatment is the principal therapeutic intervention. In 2014, over 3.6 million cataract surgeries were performed in the United States, and over 20 million surgeries were performed globally. Age-related cataracts are caused by a variety of stress conditions including elevated oxidative stress, increased sugar (diabetes), smoking or environmental insults such as exposure to ultraviolet (UV) radiation. Thus, characterization of biological and environmental factors that affect lens transparency is the first critical step toward the development of new therapies for cataracts. Recent discoveries have revealed a surprising link between proteins that are components of cytoplasmic RNA granules (RGs) and mammalian cataract. RGs like Processing Bodies (PBs) and Stress Granules (SGs) represent specialized cytoplasmic sites for regulation of RNA in the control of gene expression. PBs, the constitutive class of RGs, are RNA-protein complexes that silence or channel mRNA to decay, and therefore function to regulate the cellular proteome. SGs form as an early reaction to cellular stress, specifically allowing the translation of proteins that function in homeostasis. To investigate RG

function in lens cells, we molecularly characterized two human lens epithelial cell lines (LECs), SRA01/04 and HLE-B3. These previously uncharacterized cell lines can serve as valuable *in vitro* tools for investigating the intricate molecular basis for human cataractogenesis. It is important in cell culture studies to validate the origin and identity of the cell line. Therefore, our first step was to confirm that the cell lines were of human origin. Analyzing genome-specific Short Tandem Repeats by PCR, we authenticated that the LEC lines are indeed human-derived. We next analyzed gene expression in these LECs by high throughput Illumina microarray analysis to investigate the extent of their retention of lens-like character. The microarray data demonstrates that both LECs retain expression of genes that are expressed and/or enriched in normal lens epithelial cells. Using a bioinformatics tool "*iSyTE*" developed to predict genes implicated in lens biology and cataract, we further validated the expression of cataract associated genes in these LECs using RT-PCR. Furthermore, we find that both LECs support formation of RGs, and exhibit formation of SGs under various stress conditions such as chemical and UV-stress. Thus, these studies present the first cellular models for investigating the molecular biology of UV-radiation exposure in lens epithelial cells, and therefore represent a new resource for study of factors that are linked to age-associated cataract in humans.

Chapter 1

INTRODUCTION

1.1 The Mammalian Optic Lens

The mammalian optic lens allows mammals the evolutionary advantage of high resolution vision. The optic lens, located in the anterior of the eye, between the aqueous and vitreous humors (Figure 1.1.1A), focuses incoming light entering from the pupil onto the photoreceptors of the retina. Light incoming towards the eye is first refracted by the cornea, then by the lens. This act of refraction maximizes the photons that reach the retina, increasing the amount of visual information that the eye can perceive. The lens is a clear, non-innervated, avascular tissue that is controlled by the surrounding ciliary muscle. The subtle morphological changes imparted by the ciliary muscle allows the lens to accommodate light from varying focal lengths, thereby allowing the eye to focus on objects of varying distances (Toates, 1972). Thus the most important functional characteristics of the lens are: A) transparency, to refract and focus light on to the retina, and B) malleability, to be flexible enough for the ciliary muscle to manipulate. Loss of either of these characteristics results in loss in visual acuity.

The adult lens is comprised of two cell types, epithelial and fiber cells (Figure 1.1.1B). The difference in these cells is best understood when the lens is approached developmentally. The lens is derived from the ectoderm, where the lens placode, a thickened sheet of epithelial cells, progressively invaginates to form the lens pit, which then separates from the surface ectoderm to form the spherical, hollow lens

vesicle. The cells in the posterior of the newly formed lens vesicle cease proliferation in order to elongate, stretching themselves up toward the anterior cells that remain cuboidal and continue proliferating in a monolayer. The anterior and posterior subpopulations of cells in the lens vesicle are the precursors for the lens epithelium (anterior) and primary fiber cells (posterior). Interestingly, the fate of eptihelial cells can be modulated, as can be observed from surgical anterior-posterior reversal of the embryonic lens, which results in the once anterior epithelial cells differentiate into fiber cells based on their newly acquired posterior position (Coulombre & Coulombre, 1963). Although the transition of epithelial cells to fiber cells is a multifaceted process under the control of many signals and regulators (Blakely et al, 2000), the differentiation of epithelial cells into fiber cells at the lens equatorial region is facilitated largely by signaling through the FGF pathway, mediated by the high levels of FGF in the vitreous humor (McAvoy et al, 1999; Lovicu et al, 1989; Chamberlain et al, 1997).

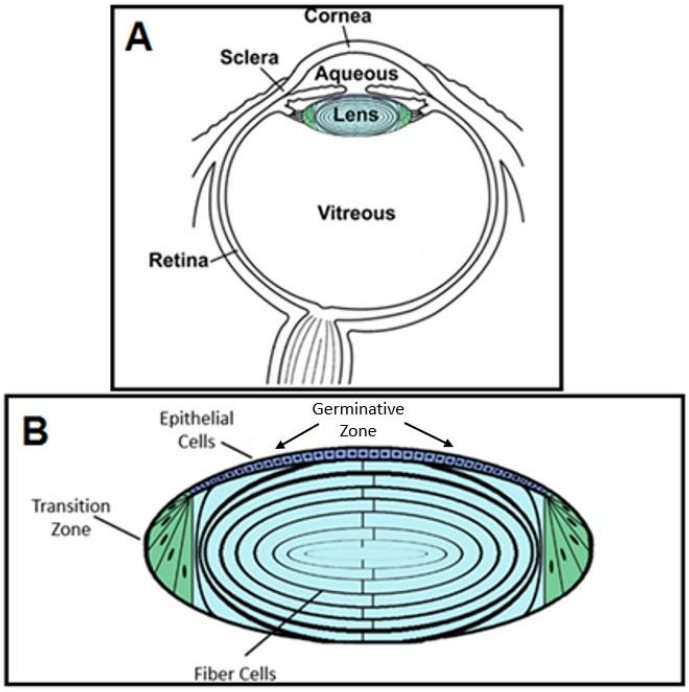

Figure 1.1.1: Organization of the lens. A) The optic lens is located in the anterior portion of the eye posterior to the aqueous humor and anterior to the vitreous humor B) Lens epithelial cells proliferate in the anterior portion of the lens, then divide and migrate to the transition zone where they differentiate into transparent enucleated fiber cells (adapted from Beyer and Berthound, 2014)

When the primary fiber cells fully elongate, they reach the apical regions of the anteriorly localized epithelial cells and fill the once hollow lens vesicle. The epithelial cell population remains in the cell cycle and continues to germinate and proliferate in a specific region called the germinative zone, in turn forcing posteriorly localized epithelial cells to pass the equatorial zone into the “transition zone”. Here, epithelial cells exit the cell cycle and initiate a terminal differentiation program to “transition” into secondary fiber cells. Bordered by secondary fiber cells, the primary fiber cells initiate the process of organelle degradation, the defining step in generating the

transparency of the lens. The process of organelle degradation is a rapid, concerted process, with its epicenter at the core of the primary fiber cells expanding the organelle free zone (OFZ) into the secondary fiber cells at a rate of 20 cell widths per day (Bassnett and Beebe, 1992). With this, the lens is fully differentiated into two distinct cell types, a proliferative minority of epithelial cells that transition into the enucleated, elongated majority of transparent fiber cells. The epithelial cells remain proliferative at the germinative zone (arrows in Figure 1.1.1B), continuing to differentiate into cortical secondary fiber cells for the remainder of the life of the lens (Zamipighi et al, 2000). In order to orchestrate the complex development and continual differentiation of the lens, lens cells are under the complex control of epigenetic mechanisms (Cvekl & Duncan, 2007), transcriptional regulators (Ogino et al, 2012), post-transcriptional regulators (Lachke & Maas, 2011, Dash et al. 2016, in press), and protein chaperones (Kumar & Reddy, 2009). Disruption or dysfunction of these precisely concerted pathways can lead to pathology of the lens and severe visual disorders.

1.2 Cataract: The World's Leading Cause of Blindness

The most prevalent pathology of the lens is cataract, the opacification or loss of transparency of the lens. Cataract causes the lens to scatter light instead of focusing it, leading to severe visual impairment, and eventually blindness (Figure 1.2.1). In addition to being the most prevalent lens pathology, cataract is also the leading cause of blindness globally, accounting for 48% of blindness worldwide (Foster & Resnikoff, 2005). According to the National Eye Institute (NEI), by age 80, more than 50% of Americans have had a cataract (NEI, 2016a). The NEI also reports that cataracts are a growing national concern, especially with an aging population, and that

the incidence of cataracts will increase from 24.4 million cases in 2010 to 38.7 million cases by 2030 (a 57% increase) (NEI, 2016b). While promising new approaches to treating cataract have been proposed in the last year (Zhao et al, 2015; Hayashi et al, 2016), surgical intervention is the only current treatment option for cataract, costing over $6.8 billion per year in the United States alone (Brown et al, 2013). Therefore, it is important to identify the molecular mechanisms underlying cataract pathology, as this represents the first step towards developing less invasive therapies for its prevention and treatment.

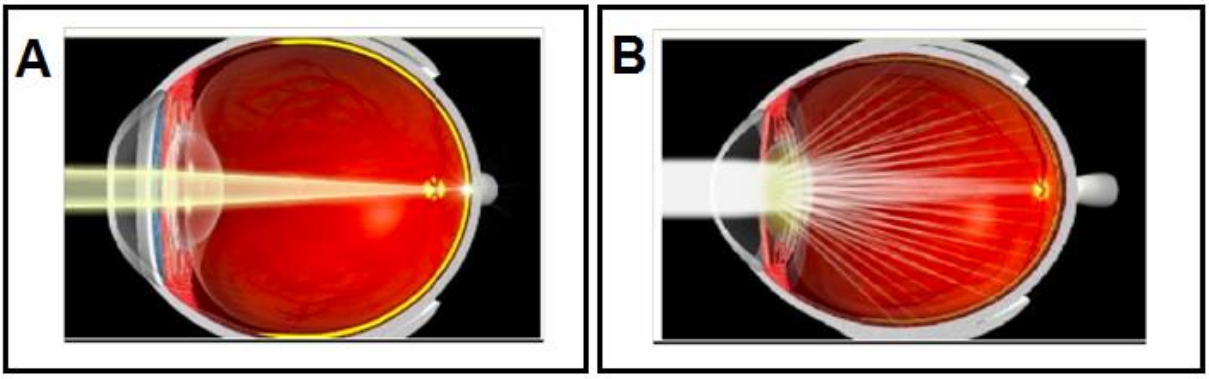

Figure 1.2.1: The lens functions to focus light on to the retina. A) A clear healthy lens functioning to focus light directly on the fovea of the retina B) A lens with cataract scattering incoming light throughout the vitreous humor, causing glare and blurred vision, as well as a yellow tint (due to the yellowed tint of the lens)

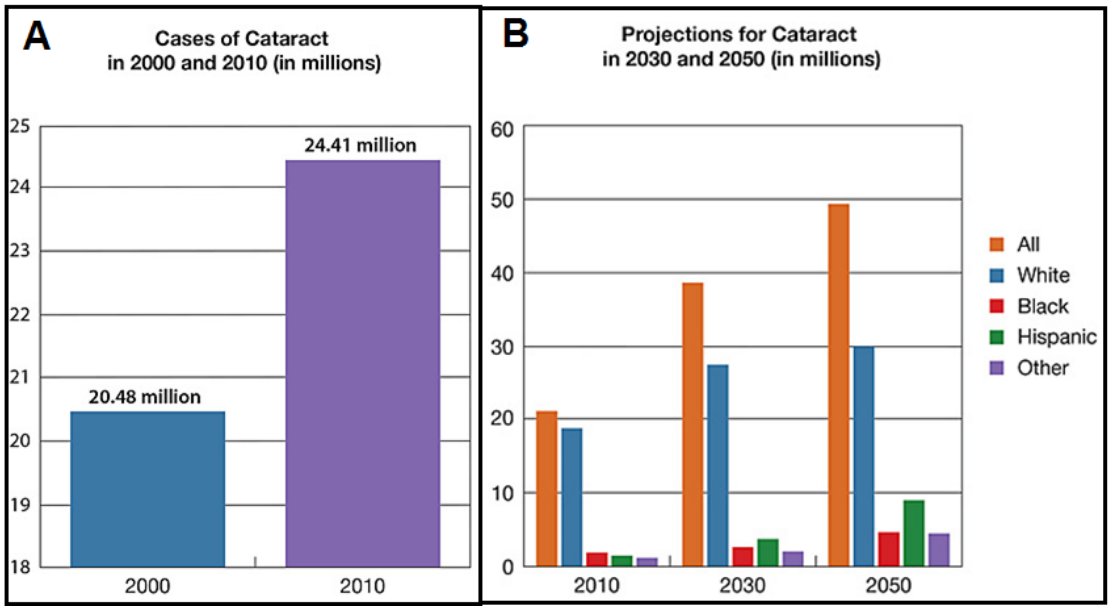

Figure 1.2.2: Incidence of Cataract in the United States. A) Data from the National Eye Institute shows that cataract prevalence has increased almost 20 percent in the United States in the last 10 years B) The National Eye Institute projects that there will be 38.7 million cases of cataract in the United States by 2030, and 50.2 million cases of cataract in 2050, a growing concern (National Eye Institute, 2012)

The opacification of the lens can be caused by several factors that affects lens cell differentiation and aggregation of crystallin proteins, among others (Nishimoto et al, 2003; Michael and Bron, 2011; Lovicu & Robinson, 2004). The etiology of these errors is the chief differentiator between the two main categories of cataract: congenital, and age-related. An estimated 25-50% of congenital cataract cases are caused by genetic mutations that alter lens development and fiber cell differentiation. Age-related cataracts, on the other hand, are far more prevalent and chiefly affect the elderly. Genetic make-up also plays a role in age-related cataracts, along with environmental insults (such as Ultraviolet (UV) Radiation and mechanical damage to

the lens), nutrition, diabetes, high cholesterol, and even use of certain drugs (Asbell, 2005).

Protein aggregation and misfolding is one of, if not the most, important factors in the formation of age-related catracts (Moreau & King, 2012). Crystallins are the proteins most highly implicated in aggregation, as they comprise 90% of the water-soluble proteins in the lens (Andley, 2012). Two crystallin families exist in the lens: α-crystallins, which are molecular chaperones whose chief function is to prevent protein aggregation, and βγ-crystallins, which are structural proteins whose high concentration and precise, tight packaging lend the lens its transparency by minimizing light-scattering (Horwitz, 1999; Benedek et al, 1999). Due to their high expression and enrichment in the lens and close proximity to one another, as well as their roles in development and maintenance of the lens, proper crystallin function is essential for lens transparency. Fifteen mutations in crystalline genes have been implicated in congenital human cataracts, denoting the importance of these proteins in lens transparency (Andley, 2012).

1.3 Predicting Cataract-Associated Genes

As of 2010, crystallin encoding-genes comprised 11 of the 22 genic mutations known to be associated with non-syndromic cataract (mutations in which cataract is the predominant phenotype) in humans (Shiels et al, 2010). However, as cataract is a multifaceted disorder resulting from the pathology of various pathways, deficiency in far more than the 22 genes identified is considered to contribute to its molecular pathology. With the advent of high-throughput technologies allowing researchers to map genomes, transcriptomes, and proteomes with greater speed and precision, researchers now have more raw data than ever on the genetic basis of cataract.

Recently, bioinformatics-based tool or databases have been developed in order to efficiently and effectively analyze this data and parse out the most promising candidates for cataract research. CatMap (http://cat-map.wustl.edu/) is an online reference database that stores genes implicated in congenital and age-related cataract in both humans and mice (Shiels et al, 2010). The number of cataract associated genes in CatMap has leapt from the 22 genes cited in the original 2010 paper to 562 genes listed by 2016 (Shiels et al, 2010; Shiels, 2016). This is a testament to both the exponential growth of technology in the field, but increased emphasis on determining the molecular basis for cataract.

The predictive tool, *iSyTE* (integrated Systems Tool for Eye gene discovery, http://bioinformatics.udel.edu/Research/iSyTE), uses comparative gene expression profiles to prioritize genes relevant to lens biology based on the enrichment of transcripts in the mouse lens compared to the whole embryonic tissue datasets (Lachke et al, 2012). This strategy of using tissue-specific enrichment as opposed to only absolute expression level is termed "whole-embryo body *in silico* subtraction" (Anand & Lachke, 2016). *iSyTE* has been used as a tool for prioritizing candidate genes linked to cataract, and has been successful in identifying in several new genes associated with cataract or lens defects: *Tdrd7*, *Pvrl3*, *Sep15*, *MafG*, and *MafK* (Agrawal et al, 2015; Dash et al, 2015; Kasaikina et al, 2011; Lachke et al, 2012; Lachke et al, 2011).

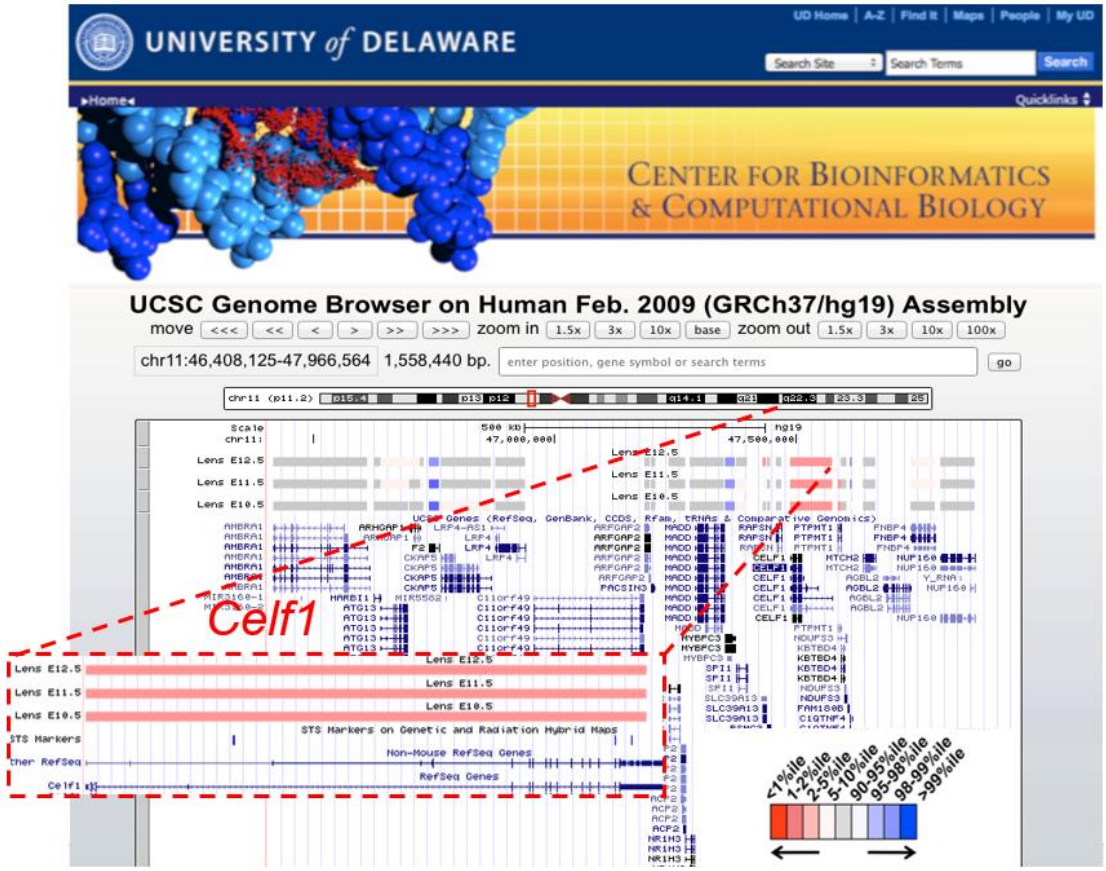

Figure 1.3.1 Identification by *iSyTE* of *Celf1* as a highly len-enriched gene. *iSyTE* predicted Celf1, an RNA binding protein highly enriched in the embryonic mouse lens, as a novel gene associated with cataract

1.4 RNA Granules and Cataract

A particularly novel cataract-associated gene predicted by *iSyTE* is *Tdrd7*, a Tudor domain and OST-HTH/Lotus domain containing RNA-binding protein (RBP). This was the first RBP to be implicated in cataract formation, and its deficiency was shown to produce cataract in human, mouse and chicken, indicative of its conservation in vertebrate lens development (Figure 1.4.1) (Lachke et al, 2011). This newfound role of *Tdrd7* in relation to cataract opened up an entirely new perspective on the

importance of RBPs, and post-transcriptional control of gene expression, in lens development, function and pathology. Since the discovery of *Tdrd7*, other RBPs such as *Caprin2* and *Celf1* have also been implicated in lens pathology and development (Dash et al, 2015; Siddam et al, in prep). The recent discovery of these genes highlights the essential role of RBPs in lens tissue.

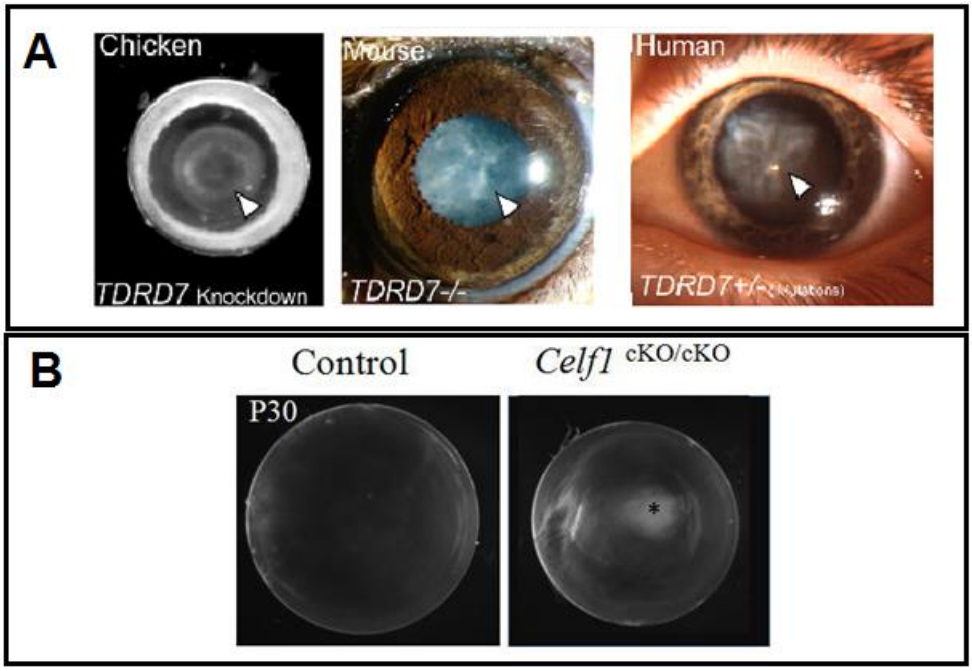

Figure 1.4.1: Conserved function of Tdrd7 in vertebrate lens development. A) Deficiency of the RNA binding protein and RNA Granule (RG) component Tdrd7 causes cataract in chicken, mice, and humans, indicative of its conserved important function in maintaining lens transparency across diverse vertebrate species B) Deficiency in *Celf1*, a second RNA binding protein and RG component, as predicted by *iSyTE*, causes cataract in the P30 mouse lens (A: Lachke et al, 2011, B: Siddam et al, *in prep*)

RBPs like *Tdrd7* are crucial influencers of post-transcriptional regulation, as they are involved in every step of the life of an mRNA. RBPs influence pre-mRNA processing (splicing, capping, polyadenylation), mRNA localization and transport, maintaining mRNA stability, mRNA error recognition (like nonsense mediated decay (NMD)), translation of mRNA into proteins, and mRNA degredation (Glisovic, 2008). 860 RBPs have been identified, characterized by over 40 RNA binding domains that allow the proteins to interact with their target mRNAs, often to a high level of sequence specificity (Castello et al, 2012). RBP dysfunction has been implicated in 15 human diseases, including myotonic dystrophy, adult onset muscular dystrophy, and fragile X syndrome, in addition to RBP misregulation being implicated in a variety of cancers (Lukong et al, 2008).

Huge complexes of RBPs, ribonucleoprotein proteins (RNPs), and mRNA in the cytoplasm, called RNA Granules (RGs), serve as the cell's main machinery for transcript storage, localization, and decay (Anderson & Kedersha, 2007). RGs are dynamic sites of post-transcriptional regulation and are classified based on function into 4 categories: processing bodies (PBs), stress granules (SGs), transport RNP particles, Neuronal Granules (NGs), and germ cell-specific granules (GCG) (Anderson & Kedersha, 2006; Lachke & Maas, 2011). PBs and SGs serve as post-transcriptional regulators universally in somatic cells throughout the body (including the lens), whereas transport RNP particles are restricted to neurons, oocytes, and fibroblasts, NGs are expressed only in neurons, and GCGs are specific to germ cells (as the name would imply) (Lachke &Maas, 2011; Anderson & Kedersha, 2006).

PBs are the constitutive class of RGs, first identified as the cytoplasmic sites for 5'-3' mRNA decay by the peculiar "granular" localization of the 5'-3' exonuclease

XRN1 (Bashkirov, 1997). It is now known that PBs contain not only the machinery for 5'-3' mRNA decay, but also the cellular machinery for RNA-induced silencing (e.g. microRNA & argonaute) and nonsense-mediated decay (Anderson & Kedersha, 2007). While PBs are present in unstressed somatic cells, additional PB assembly is induced in response to oxidative stress (Kedersha et al, 2005). The path of an mRNA through a PB begins with the dissociation of poly(A)-binding protein 1 (PABP1) bound to the the 3' end of the transcript from elongation and initiation factor 4G (eIF4G) bound to the 5' end of the transcript in the polysome, thereby linearizing the circle of the polysome transcript (Figure 1.4.2 left pathway) (Anderson & Kedersha, 2009). The translational polysome is fully converted into a PB constituent when the ribosomes run off the linearized mRNA, the transcript is de-adenylated (by the CCR4-NOT1 complex), and the "decapping" machinery binds to the transcript. This decapping machinery is a canonical constituent of PBs, comprised of Decapping Proteins 1 and 2 (DCP1, DCP2), Enhancer of mRNA-decapping protein 3 (EDC3), human enhancer of decapping large subunit (HEDLS), and DEAD-box helicase 6 (Ddx6) (Yamashita et al, 2005). These PB constituent complexes aggregate mainly through the Q/N-rich prion-related domain of EDC3, inciting the separate complexes to gather together, forming the characteristic granules (Reijns et al, 2008). From the granular stage, PBs can degrade transcripts after decapping, or simply sequester the transcripts temporarily for later re-initiation of translation (a decision possibly mediated by eIF activity) (Gimenez-Barcons & Diez, 2011).

SGs are the inducible class of RGs, assembled in response to various cellular stressors. SGs were first identified as "Heat Shock Granules", preferentially binding housekeeping protein transcripts, and excluding the transcripts of heat shock proteins

in heat-stressed cells (Nover et al, 1989). SGs are now known to form in response to a wide range of causes, including: a variety of environmental stress (heat shock, hypoxia, UV irradiation, oxidative stress), inhibition of translation initiation, overexpression of certain RBPs, and *en masse* dissociation of mRNAs from ribosomes (Buchan, 2009). The phosphorylation of the polysome constituent eIF2α by any number of stress-sensing serine/threonine kinases is the inciting step in the assembly of SGs (Kedersha et al, 1999). Phosphorylating eIF2α inhibits the formation of the eIF2/$tRNA_i^{met}$/GTP ternary complex thereby inhibiting the initiation of translation and translationally stalling the small ribosomal subunits bound to mRNA (Kedersha et al, 2013). Unlike in PBs, the transcripts within SGs remains circularized through the binding of the eIF3 subcomplex to phosphorylated eIF2, the small ribosomal subunit, and eIF4G, thus keeping the 5' cap and 3' poly(A)-tail in close proximity (Jivotovskaya, 2006). Keeping the mRNA circularized, adenylated, and attached to the small ribosomal subunits allows SGs to more quickly sequester mRNA from stress and to more quickly transition back into functioning translational polysomes. The stalled circularized transcript complexes are then bound by proteins that stabilize the mRNA and further silence translation: T-Cell Restricted Intracellular Antigen-1 and R (TIA1, TIAR), and GTPase-activating protein SH3 domain binding protein (G3BP) (Anderson & Kedersha, 2009). All three of these proteins are self-aggregating, with TIA-1 and TIAR containing Q/N-rich prion-related domains similar to EDC3 in PBs (Gilks, 2004). Just as in PBs, these self-aggregating proteins cluster the individual stalled-translation complexes into large SGs.

Much of our current knowledge on both PBs and SGs comes from experiments in the yeast *Saccharomyces cerevisiae*. Experiments on various stressors of

Saccharomyces showed that different stressors elicit different proteins to be recruited by both SGs and PBs (Buchan, 2011). These differential protein compositions are fundamental to the stress response, as they determine which transcripts the RGs will sequester and degrade, and thus which transcripts will be expedited through translation to aid in returning the cell to homeostasis. The formation of SGs promotes cell survival not only through sequestering housekeeping transcripts, but also by sequestering pro-apoptotic proteins and delaying apoptotic signals. During oxidative stress conditions including hypoxia, and arsenite stress, SGs have been shown to negatively regulate the SAPK apoptotic response by sequestering the signaling protein RACK1, and interrupting the kinase cascade that would lead to programmed cell death (Wang et al, 2015). Thus, not only do SGs form to maintain the homeostasis of the cell, but SGs actively function to maintain pro-life signals and stave off premature cell-death.

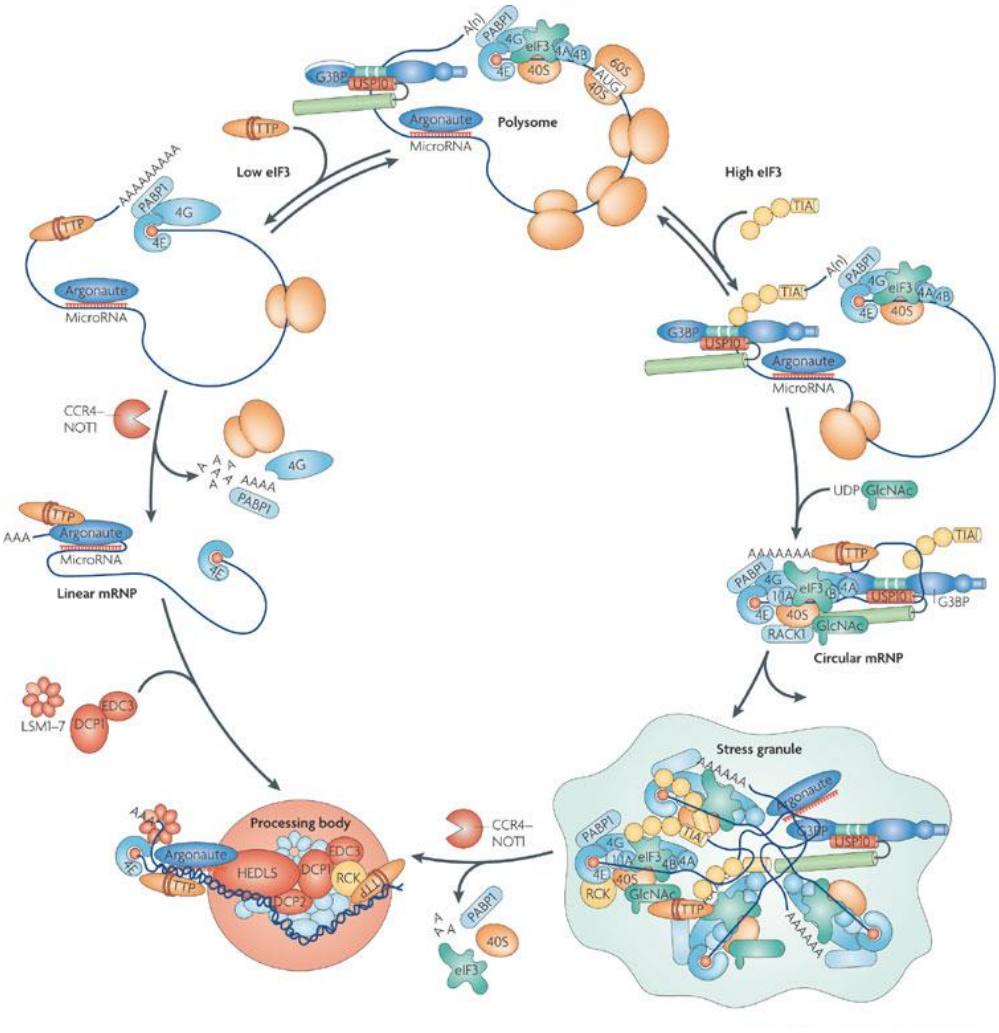

Figure 1.4.2: Processing bodies and Stress granules. The two types of RNA granules important to post-transcriptional regulation in the lens, Processing bodies (left linearization pathway) and Stress Granules (right circularization pathway). This diagram notes eIF3 as one of the chief drivers of Stress Granule formation (Anderson & Kedersha, 2009)

1.5 UV, the Lens, and RNA granules

Recent epidemiological meta-studies have implicated stress from UV radiation as a culprit for cataract formation (Midelfart, 2005; Dolin, 1994). Additionally, in an epidemiological survey of over 800 dock workers on the Chesapeake Bay, doubled UV exposure increased the workers' risk for cataract by a factor of 1.6 (Taylor, 1988). While studies have shown induction of cataract through UV radiation *in vivo* in guinea pigs, rats, mice, and cows no study has linked the UV stress response in the lens to RNA granules (Kakar, 2004; Zhang, 2012; Ayala, 2000; Malina, 1995). Recent studies have linked UVC radiation (the highest frequency, and most energetic form of UV) to the formation of Stress Granules in the mouse fibroblast cell line NIH-3T3 (Moutaoufik, 2014). Additionally, HeLa cells have been shown to respond to UVC-irradiation with Stress Granules and miRNA gene silencing hours after irradiation (Pothof, 2009). However, UVC is not a biologically relevant stressor of the lens, as studies have shown that the cornea absorbs light of wavelengths less than 295nm (Barker, 1991; Roberts, 2001). Only UVB (300-315nm) and UVA (315-400nm) penetrate through the cornea to reach the lens, with the cornea absorbing 60%-100% of UVB, and 20-40% UVA (Hammond et al, 2014). UVB has been shown to activate members of the SG pathway (ROCK1 and TIAR) in human and mouse keratinocytes, however SGs have not been directly implicated in the cellular response to UVA or UVB exposure (Ongusaha, 2008; Tong et al, 2007).

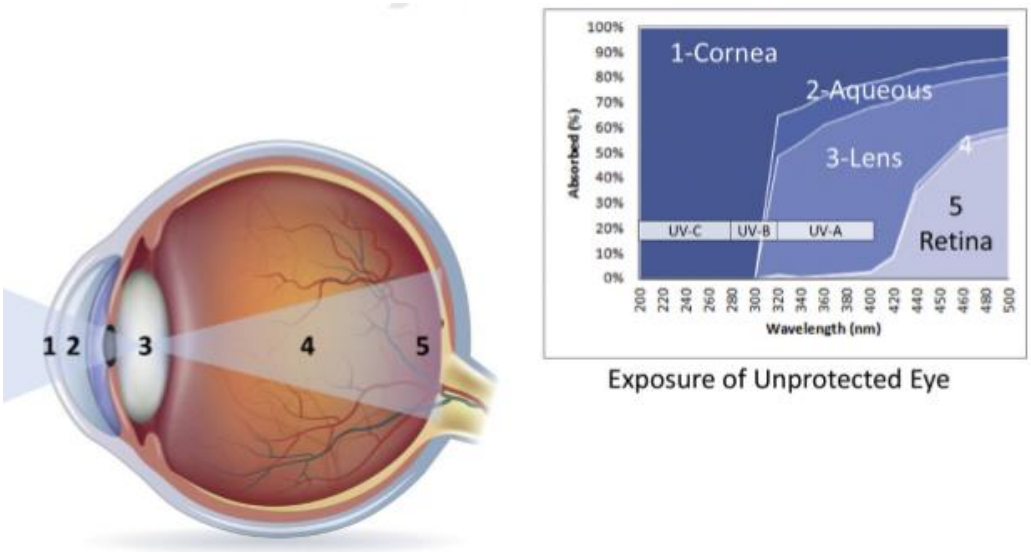

Figure 1.5.1: The penetration light through the eye as a function of wavelength. The lens absorbs 40% of longer wavelengths of UVB and most of the UVA that enters the eye (adapted from Hammond et al, 2014)

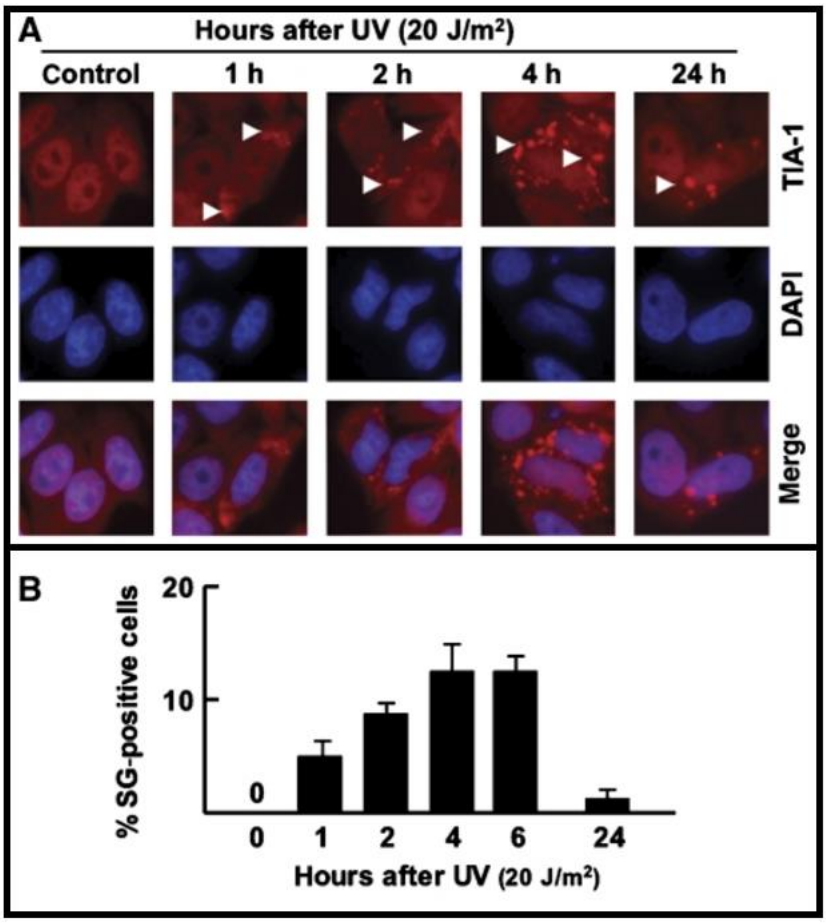

Figure 1.5.2: HeLa Cells stressed with UVC exhibit stress granules hours after irradiation. TIA-1 was used as a stress granule marker. HeLa cells were shown to recover significantly from the stress after 24 hours (Pothof, 2009)

1.6 Cell Lines and In Vitro Models for the Human Optic Lens

Cell lines are secondary cultures of specific tissue immortalized so that the tissue can be cultured and passaged for long periods of time (possibly indefinitely). Cell lines are valuable tools for biological research, as they allow for more precise manipulations and assays of cells than *in vivo* studies, avoid the ethical issues of

testing on animal subjects, and provide a (functionally) endless supply of pure tissue with reproducible results (Kaur & Dufour, 2012). The American Type Culture Collection maintains almost 4,000 human cell lines as well as cell lines from over 150 species, denoting the widespread use of cell lines in biomedical research (ATCC, 2016).

Two such cell lines exist for human lens epithelial cells (LEC), HLE-B3 (sold by the ATCC as B-3 http://www.atcc.org/products/all/CRL-11421.aspx) and SRA01/04. Combined, the cell lines have been used in over 150 publications (Figure 1.6.1) according to Pubmed. HLE-B3 was immortalized in 1994 from a 5 to 12 month old female patient whose whole eye was removed as treatment for retinopathy. The healthy lens epithelium was extracted and cultured in media, then virally infected with an adenovirus carrying the large T antigen for Simian Virus 40 (Tag SV40). The viral infection immortalized the epithelial cells by disallowing the cells to exit the cell cycle, thereby continuously regenerating while never differentiating into post-mitotic fiber cells (Andley et al, 1994). SRA01/04 was immortalized in 1998 from an infant male patient who also underwent treatment for retinopathy. SRA01/04 was transfected with Tag SV40 using a plasmid vector, marking the chief difference between the two cell types (Ibaraki, 1998). Combined, both cell lines have been used in 155 studies (Figure 1.6.1) according to PubMed. Several studies have tested the effect of UVA on HLE-B3 (Xi et al, 2003), UVB on HLE-B3 (Heo et al, 2008; Shin et al, 2004; Obrenovich et al, 2006; Andley et al 1996), UVB on SRA01/04 (Osada, 2011; Yao, 2008; Sachdey, 2004; Shui, 2000), and UVC on SRA01/04 (Okuno, 2007).

However, despite the prevalence of HLE-B3 and SRA01/04 in lens research, neither cell line has been validated for its lens-like character and overall expression of

lens-enriched genes. The only attempts to validate lens-like characteristics in the cell lines during the immortalization procedures was western blotting for βH-crystallin and γ-crystallin in HLE-B3, and RT-PCR for *CRYAA* and *CRYBB2* in SRA01/04. Since its immortalization, only one study has analyzed the proteome of HLE-B3 through low-throughput analysis, reporting a marked reduction in all crystallins (except αB-crystallin) and aldose reductase when comparing HLE-B3 to protein extracts of *in vivo* human lens epithelial and fiber cells (Wang et al, 2003). In order to uphold past studies and approve future studies on these cell lines, their aptitude to serve as models of the human lens must be thoroughly assessed.

The lack of validation and authentication of cell lines has come under particular scrutiny in recent years. Authentication refers to the practice of confirming the species of origin of the cell line in question, usually through assays of genomic DNA. The eye research community in particular has voiced an outcry for authentication of cell lines to prove their species of origin. Any cell lines used in studies submitted to three major journals in eye research must now be authenticated, according to statements released by the editors (Beebe, 2013; The Editors of Molecular Vision, 2013; The Editors of Experimental Eye Research, 2013). This mandate came on the heels of the disastrous discovery that the widely used rat Retinal Ganglion Cell line RGC-5, was not, in fact the cell line it claimed to be. Not only was the cell line exposed as a mouse cell line, but RGC-5 also did not express retinal ganglion cell markers, and, in fact, matched the exact genetic identity of the mouse photoreceptor line 661W (Krishnamoorthy et al, 2013). In addition to cell line scandals such as RGC-5, the ATCC has discontinued the use and distribution of 29 of its human cell lines due to Short Tandem Repeat profiling discrepancies, including six

human cell lines discontinued for “inappropriate Y” results in cells of putative female origin (ATCC, 2016).

Short Tandem Repeat (STR) analysis has become the gold standard for authentication due to its minimal cost, high specificity, and ability to use technology already available to many labs. STRs, also called microsatellites, are sequences of genomic DNA where small sequences (between two and seven nucleotides) are repeated contiguously (Chambers& MacAvoy, 2007). STR Analysis uses primers directed to known STRs at specific chromosomal loci to amplify that specific STR locus. In this study, the primers were designed to amplify specific Short Tandem Repeat patterns found only in humans in specific loci on 12 different human autosomal chromosomes. These STR loci are a consensus sequences chosen to be the Combined DNA Index System (CODIS) core STR loci, used internationally for human cell line authentication, as well as by the FBI for DNA profiling in the National DNA Index System (NDIS) (Miller et al, 2003; Butler, 2006). The American Type Culture Collection uses 8 of the 13 CODIS loci to authenticate their own cell lines (Masters, 2001; Masibay et al 2000). Each of the 13 CODIS STRs are so chosen because of their location on distinct chromosomes, tetrameric repeat pattern, and low incidence of mutation (Ruitberg, 2001).

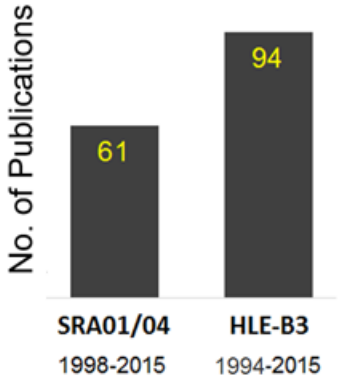

Figure 1.6.1: Graphic of the total publications of both human LEC lines

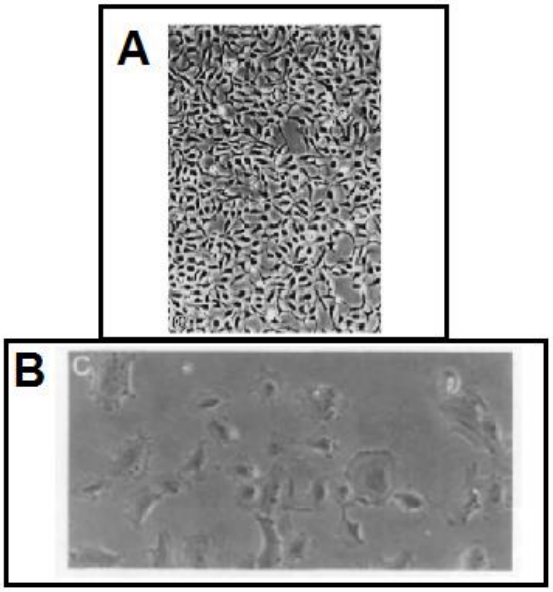

Figure 1.6.2 The human lens epithelial cell lines SRA01/04 and HLE-B3 A) Phase contrast micrograph of SRA01/04 cells grown in serum-free media B) Phase contrast micrograph of HLE-B3 2 days after the first passage (A: Ibaraki et al, 1998, B: Andley et al, 1994)

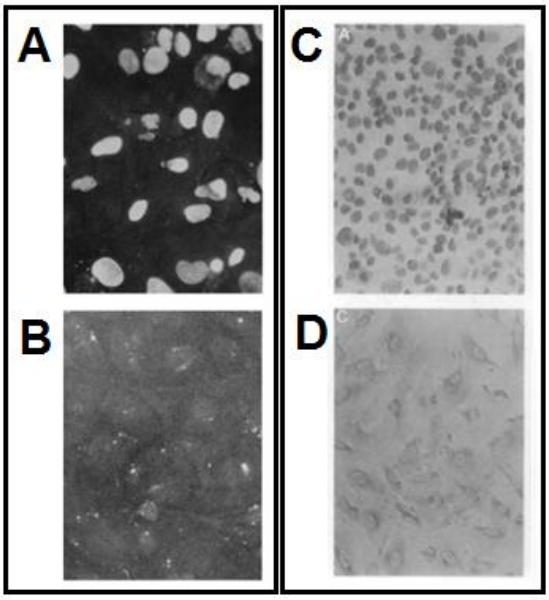

Figure 1.6.3: Fluorescence micrographs of cells treated with mouse anti-SV40 antibodies A&B) SRA01/04 cells with distinct fluorescent nuclei(A) compared to non-transfected controls (B) C&D) HLE-B3 cells with distinct fluorescent nuclei (C) compared to non-infected controls (D) (A&B: Ibaraki et al, 1998; C&D: Andley et al, 1994)

Chapter 2

MATERIALS AND METHODS

2.1 Cell Culture

The HLE-B3 cell line was obtained from the American Type Culture Collection (ATCC) and SRA01/04 was generously provided to Lachke lab directly by Professor Venkat Reddy (Oakland University, Michigan), who originally derived this cell line. HEK293T cells were used as a comparative cell line and were a generous gift from Donna Woulfe's Lab. All the cell lines were cultured in 100mm cell culture plates (Eppendorf) in 10 mL of: Dulbecco's Modified Eagle's Medium (DMEM) 1x with 4.5 g/L glucose, L-glutamine, and sodium pyruvate (Corning), 10% Fetal Bovine Serum (Fisher Scientific), and 1% penicillin-streptomycin (GE Healthcare Life Sciences). The cells were incubated at 37°C in a humid chamber with 5% CO_2. All cell lines were passaged at least three times after freeze-thaw before RNA isolation, DNA isolation, stressing, or immunostaining.

2.2 Authentication of Cell Lines

Cell lines were authenticated using Short Tandem Repeat (STR) analysis to ensure that each cell line was human in origin. Genomic DNA was extracted from four cell lines (SRA01/04, HLE-B3, HEK293T, and the mouse lens epithelial cell line 21EM15) using the Gentra Puregene Core Kit A (Qiagen).

Primers directed towards mouse STRs were used as a negative control. Sequences for human CODIS STR primers were obtained from Azari et al, 2007, and sequences for mouse STR primers were obtained from Almeida et al, 2014. Table 2.2 lists all primers used in authentication.

Human STR locus	PCR primer sequences	Product size (bp)	Chromosomal location
CSF1PO	(F)AACCTGAGTCTGCCAAGGACTAGC	291–331	5q
	(R)TTCCACACACCACTGGCCATCTTC		
FGA	(F)GCCCCATAGGTTTTGAACTCA	158–314	4q
	(R)TGATTTGTCTGTAATTGCCAGC		
THO1	(F)ATTCAAAGGGTATCTGGGCTCTGG	171–215	11p
	(R)GTGGGCTGAAAAGCTCCCGATTAT		
TPOX	(F)ACTGGCACAGAACAGGCACTTAGG	220–256	2p
	(R)GGAGGAACTGGGAACCACACAGGTTA		
VWA	(F)GCCCTAGTGGATGATAAGAATAATCAGTATGTG	123–181	12p
	(R)GGACAGATGATAAATACATAGGATGGATGG		
D3S1358	(F)ACTGCAGTCCAATCTGGGT	99–147	3p
	(R)ATGAAATCAACAGAGGCTTG		
D5S818	(F)GGTGATTTTCCTCTTTGGTATCC	119–155	5q
	(R)AGCCACAGTTTACAACATTTGTATCT		
D7S820	(F)ATGTTGGTCAGGCTGACTATG	211–251	7q
	(R)GATTCCACATTTATCCTCATTGAC		
D8S1179	(F)TTTTTGTATTTCATGTGTACATTCG	157–205	8q
	(R)CGTAGCTATAATTAGTTCATTTTCA		
D13S317	(F)ACAGAAGTCTGGGATGTGGA	157–201	13q
	(R)GCCCAAAAAGACAGACAGAA		
D16S539	(F)GGGGGTCTAAGAGCTTGTAAAAAG	264–304	16q
	(R)GTTTGTGTGTGCATCTGTAAGCAT		
D18S51	(F)CAAACCCGACTACCAGCAAC	262–342	18q
	(R)GAGCCATGTTCATGCCACTG		
D21S11	(F)GTGAGTCAATTCCCCAAG	202–260	21p
	(R)GTTGTATTAGTCAATGTTCTCC		
Mouse STR locus	**PCR primer sequences**	**Product size (bp)**	**Chromosomal location**
X-1	(F)GGATGGATGGATGGATGAAA	357-442	X
	(R)AAGGTATATATCAAGATGGCATTATCA		
5-5	(F)GTTTACCCCTGCATCACTGG	258-298	5
	(R)TCAGAATTGCTCATAGTGCAAGA		

Table 2.2: Primer sequences used for STR analysis. Primer sequences for each locus are listed. “F” refers to forward primers, while “R” refers to reverse primers. “p” and “q” after chromosome number refers to the p (short) or q (long) arm of the chromosome

STR regions were amplified using Polymerase Chain Reaction (PCR) with Taq PCR Core Kits (Quiagen) in a T100 Thermocycler (BioRad). For the 25µL PCR

reaction mixture, see Appendix A. The amplification program used for the human primers was: 95°C for 3 min, then 35 cycles of 94°C for 30 sec, 64°C for 45 sec, 72°C for 45 sec, followed by 72°C for 10 minutes. The amplification program used for the mouse primers was: 95°C for 3 min, then 35 cycles of 94°C for 30 sec, 60°C for 45 sec, 72°C for 45 sec, followed by 72°C for 10 minutes. The products from these PCR experiments were separated by size by electrophoresis on a 1% agarose gel with Ethidium Bromide and imaged using a GelDoc-It 310 imager (UVP).

2.3 Whole-genome dataset Analyses

Microarray datasets for HLE-B3 and SRA01/04 were generated by Dr. Lachke using the Illumina Human Ref-8 v3.0 expression beadchip. Microarray data was analyzed in 'R' Statistical environment (http://www.r-project.org/index.html). The raw data from the chip was corrected for background noise using *bjadjust* in the *lumi* package on *Bioconductor* (http://www.bioconductor.org/), and normalized with the *Rank invariant* method included in *lumi*. Gene ontology was analyzed using *Go.Db*, and Pathway analysis was conducted through *KEGG*. Three biological replicates were used, and only probes with detection p values ≤ 0.05 in two or more replicates were considered for gene-level analysis. Genes were filtered for lens-enriched genes through *iSyTE* and rank-analyzed for probe-presence.

2.4 RT-PCR and qRT-PCR Analysis

Total RNA of HLE-B3, SRA01/04, and HEK293T cell lines was extracted using the RNAeasy Mini Kit (Quiagen). The total RNA extracted was quantified using an ND-1000 nanodrop spectrophotometer (Thermo Scientific). The total RNA of each

passage of each of the three cell lines was then synthesized into cDNA in a concentration of 200ng/µL using the iScript cDNA Synthesis Kit (Bio-Rad).

Primers for RT-PCR and qRT-PCR analysis were generated using NCBI PrimerBLAST (http://www.ncbi.nlm.nih.gov/tools/primer-blast/index.cgi?LINK_LOC=BlastHome). The coding sequence (CDS) for each gene was run with Primer-BLAST using a desired product size of 100-300 nucleotides and requiring each primer to span an exon-exon junction. Primer results from Pimer-BLAST were then tested *in silico* using Sequence Manipulation Suite's *PCR Primer Stats* program (http://www.bioinformatics.org/sms2/pcr_primer_stats.html) for their percent GC content, ability to form a GC clamp, ability to self-anneal, and ability to form hairpins. Those primers that passed these tests were then assessed for specificity to their target sequence with UCSC's *In-Silico PCR* (https://genome.ucsc.edu/cgi-bin/hgPcr) using the GRCh38/hg38 Assembly to ensure the primers did not bind to genomic DNA. Primer sequences were then submitted to Integrated DNA Technologies and shipped to Lachke Laboratory as custom oligoDNAs. Appendix B lists the primers used for RT-PCR and qRT-PCR.

For RT-PCR, transcripts for target genes were amplified using Taq PCR Core Kits (Qiagen) and a T100 Thermocycler (BioRad). Each primer set was tested initially using the PCR reaction mix in Appendix A and the PCR program: 94°C for 2 minutes, then 40 cycles of 94°C for 15 seconds, 60°C for 30 seconds, 72°C for 30 seconds, followed by 72°C for 4 minutes. Each PCR product was then visualized using the same process outlined for authentication in 2.2. If the appropriate PCR product was not seen after gel electrophoresis for a certain primer set, a specific methodology for subsequent RT-PCR amplification was followed. First, the volume of cDNA was

increased to 1.0µL. If no product was detected, the number of PCR cycles was increased to 40 with the original 0.65 µL of cDNA. If the expected product was still not detected, a temperature gradient was used to achieve an appropriate melting temperature for the primer set (within 5 degrees Celcius of the primer's listed Tm), which was then used in a subsequent 35 cycle PCR. If none of these methods succeeded in generating the expected PCR product, new primers for the gene being assayed were designed and retested. RT-PCR results were compared to the housekeeping gene Beta-Actin.

For RT-qPCR (reverse transcriptase followed by quantitative PCR), each reaction was housed in a 96-well reaction plate (Applied Biosystems) and used Power Syber Green PCR Master Mix (Invitrogen Life Technology). The reaction mix used for each RT-qPCR reaction can be found in Appendix A. RT-qPCR reactions were carried out in technical triplicate and biological triplicate (cDNA from three consecutive passages) on the same plate for each cell line for each gene being assayed (a total of 9 replicates for each gene for each cell line). Each plate was analyzed on the 7500 Fast PCR system (Applied Biosystems). For each gene SRA01/04 was compared to HEK293T. Significance of fold changes were determined using two-level nested variance analysis developed by John McDonald, PhD.

2.5 Immunostaining Analysis

For *in vitro* immunostaining analysis, each cell line was first plated in a 6-well tissue culture plate (Millipore) with a 22x22 glass coverslip in each well. Cells were then grown to 70% confluence on each coverslip before stressing (see 2.6) or staining.

Both stressed and unstressed cells were washed in PBS, then fixed in 4% paraformaldehyde for 15 minutes at room temperature. Cells were then washed in ice

cold methanol for 10 minutes, washed with PBS, and blocked for one hour in blocking buffer consisting of: 1xPBS, 5% chicken serum (Abcam), and 0.3% Triton X-100. The cells were then incubated overnight at 4°C with primary antibodies in blocking buffer. The antibodies used were rabbit Ddx6 (Bethyl Labs #A300-461A) for Processing Bodies at a concentration of 1:300, and goat eIF3b (Santa Cruz #16377) for Stress Granules at a concentration of 1:200. After overnight incubation the cells were washed with PBS and incubated for one hour with secondary antibodies in blocking buffer. The secondary antibodies used were Alexa Fluor chicken anti-goat 488 and Alexa Fluor chicken anti-rabbit 594 (Life Technologies #A-11039) in a concentration of 1:500, and Draq5 (BioStatus Ltd) for nuclear staining in a concentration of 1:2000. The immunofluorescent slides were imaged with a Model 780 confocal microscope (Zeiss).

For *in vivo* immunostaining, C57/Blc6 mice at post-natal stage (P) 30 were sacrificed and the entire intact ocular tissue was isolated and embedded in OCT freezing medium for sectioning either without exposure to stress conditions, or after exposure to UV stress (see 2.6). Whole eyes were then cryosectioned into 15 µm transverse sections, scored under a light microscope at low magnification, frozen on dry ice, and stored at -80°C until staining. Immediately prior to staining, sections were immersed in 4% PFA for 15 minutes for fixation, then washed with PBS and permeabilized in ice cold methanol for 10 minutes (as with the cell lines). Frozen sections were stained using the same procedure as the cell lines. Primary antibody concentrations were increased to 1:100 for both Ddx6 and eIFb, and secondary antibody concentrations remained the same (1:500 for Alexa 594 and Alexa 488), as did Draq5 (1:2000).

2.6 Stress Conditions

The cell lines were subjected to both chemical and Ultraviolet (UV) radiation-based stress. Chemical stress in the cells was induced in by adding 20µL of 0.05M sodium arsenite (Fluka Analytical) to cells plated on coverslips in 2mL of culture solution (DMEM, 10%FBS, 1%pennicilin-streptomycin). Cells were stressed in the 0.0005 M sodium arsenite solution for 45minutes in 37°C and 5% CO_2, then proceeded immediately to PBS wash and immunostaining.

Cells were irradiated using the UVLM-26 EL Series Lamp (UVP). The lamp produced UVA at a wavelength of 365nm and a power of 1.5 mW/cm^2 (at a distance of 3 inches from the surface of the lamp) and UVB at a wavelength of 302nm and a power of 2.0 mW/cm^2 (also at a distance of 3 inches). The lamp was placed on a custom UV lamp apparatus that allowed the cells to maintain a distance of 3 inches from the lamp whilst remaining on coverslips in a 6-well culture plate. Before UV stress, cells adhered to coverslips were moved to wells in new 6-well culture plates and covered in 2 mL of 1xPBS. The cells were irradiated in a spare cell culture incubator at 37°C and 5% CO_2 for varying times, ranging from 15 minutes to 2 hours (in intervals of 15 minutes). Cells were then either immediately washed and fixed for immunostaining, or allowed to recover for up to two hours.

For *in vivo* stress, C57/Blc6 mice at stage P30 were sacrificed and their entire intact ocular tissue was isolated. The eye was then placed on top of a solidified gel made from 5% agarose in DMEM with the optic nerve facing down (and cornea facing up) and submerged in 1x PBS. Whole eyes were then stressed by UV irradiation at variable times up to 3 hours in 37°C and 5% CO_2. Whole stressed eyes were then immediately embedded in OCT, and proceeded through the immunostaining protocol.

2.7 Quantification of RNA Granules

RNA granules (RGs) were quantified using confocal images of immunostained slides taken at 40x magnification. Ddx6 was used as the Processing Body marker and eIF3b was used as the Stress Granule marker. SGs and PBs were counted using separate channels, and the level of stress for each image was blind to the counter. All counting was done using ImageJ (https://imagej.nih.gov/ij/) an image processing and analysis program available through the National Institute of Health. Each confocal image was split into three channels, and the number of RGs for each channel was counted using the ImageJ plugin "Cell Counter". At least 3 fields of view and 50 cells were counted for each stress condition. The number of total RGs was divided by the number total cells for each view, and the resulting RGs/cell was averaged for each stress condition. Statistical significance was then calculated using a student t-test with two tailed distribution through the program Prism Graphpad (http://www.graphpad.com/scientific-software/prism/).

Chapter 3

RESULTS

3.1 Human LECs Authenticated as Human-Derived cells

STR analysis of the cell lines confirmed that both HLE-B3 and SRA01/04 are of human origin, as expected, and free of any mouse origin cells. This is an important initial step as it confirmed that the cell lines were of human origin as originally described. Both cell lines showed the same STR genomic DNA profile as HEK293T cells, an estblished human cell line that served as positive control. 21EM15, the mouse lens epithelial cell line used as a negative control exhibited no PCR products for the 13 human CODIS primer sets, but strong PCR products for the two mouse primer sets used, further ensuring that the human PCR products were not false positives. Furthermore, the human cell lines showed no PCR products for the mouse STR primer sets, further ensuring that the cell lines were not also contaminated by mouse cells.

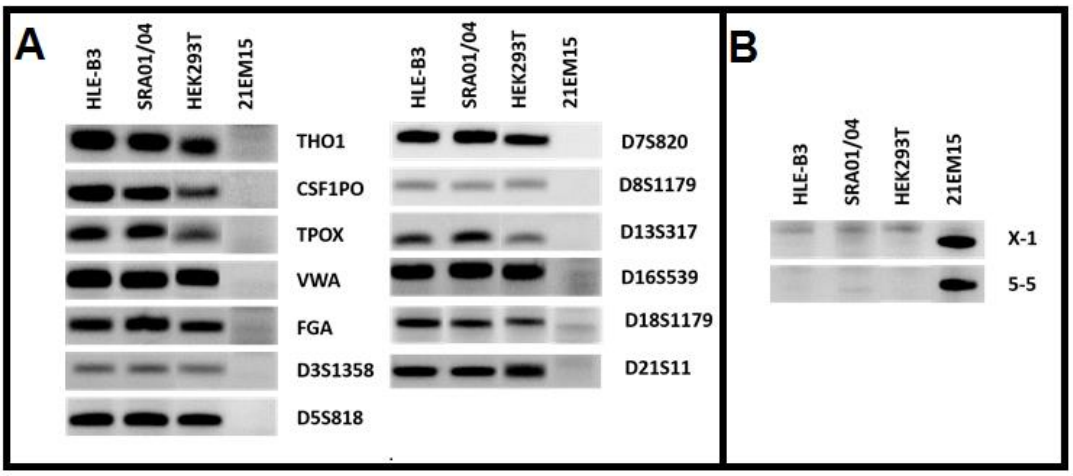

Figure 3.1.1: STR analysis of the human lens epithelial cell lines HLE-B3 and SRA01/04. STR analysis shows that both cell lines are human in origin. A) Both cell lines exhibit PCR products for all 13 CODIS loci primer sets (as does the positive control human cell line HEK293T), while the mouse cell line 21EM15 does not B) all human cell lines show no PCR products for mouse STR primer sets, while the mouse cell line does exhibit PCR products for the mouse STR primer sets.

3.2 Human LECs Show Gene Expression Profiles Similar to *In Vivo* Lenses and *In Vitro* Validated Models

The microarray data of both HLE-B3 and SRA01/04 showed that the human LEC lines had similar gene expression profiles to both *in vivo* mouse lenses and the previously validated mouse LEC line 21EM15 (Figure 3.2.1). Microarray and RNA-sequencing data of *in vivo* mouse lens epithelial cells and fiber cells generated independently by two other labs show similar expression of lens-enriched genes to the human LEC lines. Highlighted in the figure are five genes differentially expressed in the mouse LECs and *in vivo* and *in vitro* mouse lens epithelial cells. The human LEC lines express significantly less of the genes: *Gp38* (a type-1 integral glycoprotein),

Hs2st1 (Heparan Sulfate 2-O-Sulfotransferase), *Prox1* (a fiber cell-specific transcription factor), and *Hmox1* (a Heme oxygenase). *Hspb1*, a heat shock protein, was conversely found to be expressed in much greater levels in the human LEC lines.

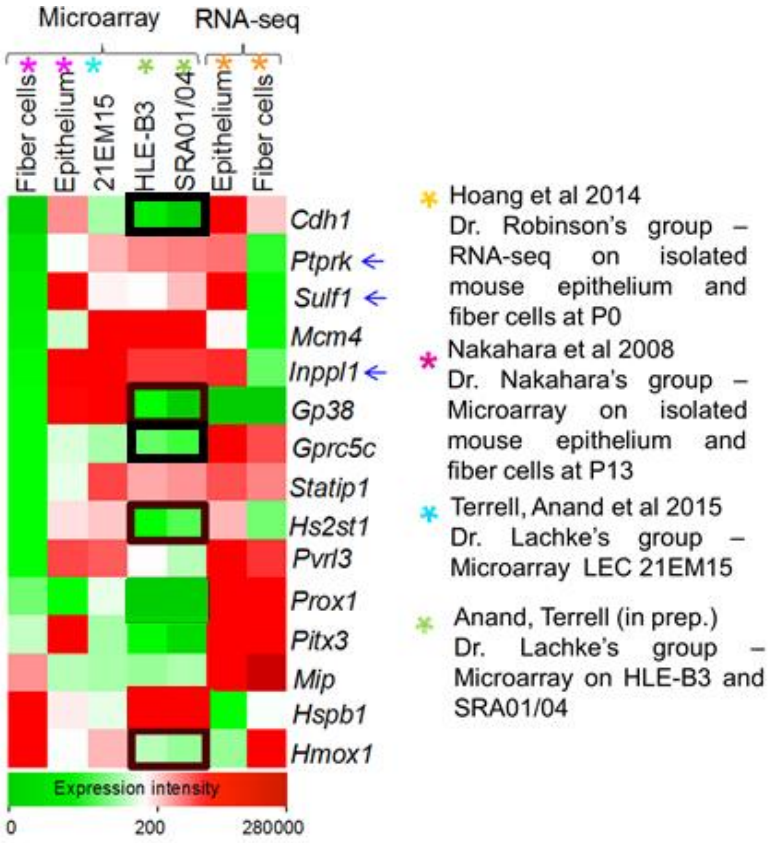

Figure 3.2.1: Comparative analysis of gene expression profiling between lens and lens epithelial cell lines. Genome-wide transcript-level analysis of the human LEC lines exhibited similarities in gene expression profiles to *in vivo* mouse gene expression profiles. Lens fiber cells and epithelial cells were analyzed by microarray and RNA-sequencing independently by two laboratories. Further, a previously validated mouse LEC line 21EM15 was also used in this comparative analysis. The few genes that are not expressed as expected in the human LEC lines are indicated by black boxes.

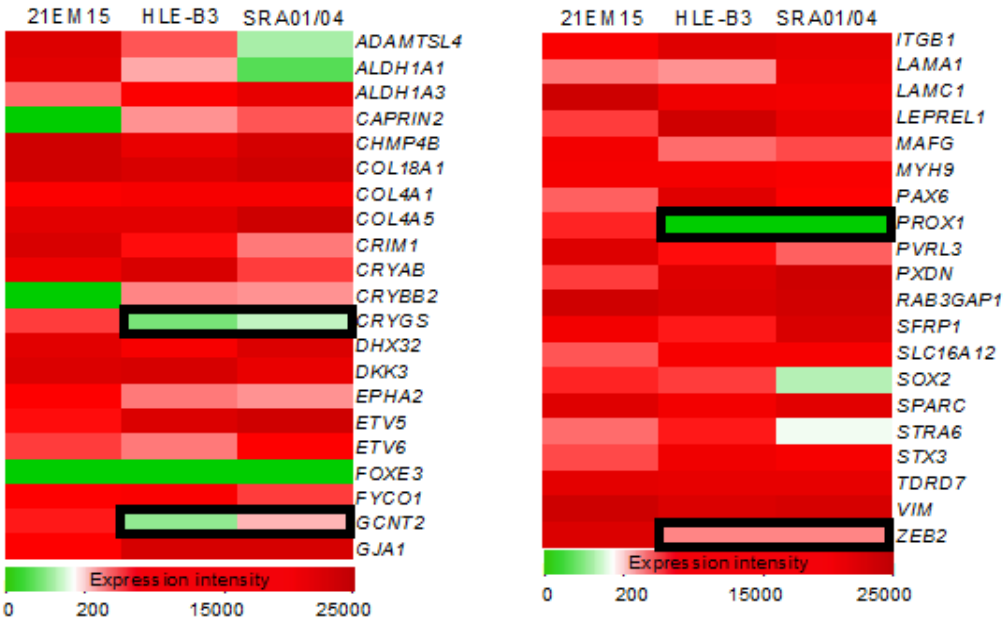

Figure 3.2.2: Comparative microarray analysis of select lens expressed genes in human and mouse lens epithelial cell lines. Genome-wide transcript-level analyses show that the human LEC lines have largely similar gene expression profiles to the mouse LEC line 21EM15. Genes expressed less highly in the human LECs than 21EM15 are indicated by black boxes. SRA01/04 shows additionally decreased expression of 4 more genes when compared to both HLE-B3 and 21EM15.

The human LEC lines have strikingly similar gene expression profiles to the previously-validated mouse LEC line, 21EM15 (Figure 3.2.2). Promisingly, the microarray data shows that the human LEC lines have increased expression of *CAPRIN2* (an RBP shown to cause developmental lens defects (Dash et al, 2015)), *GJA1* (a gap junction gene important for epithelial molecular transport and exchange (Zampighi, 2000)), and *CRYBB2* (a β-crystallin gene). Conversely, the human LEC lines exhibit decreased levels of *ALDH1A1* (an aldehyde dehydrogenase crucial to the lens's response to oxidative stress, whose mutation causes cataract (Choudhary et al,

2005)), *CRYGS* (a γ-crystallin whose mutation causes cataract (Sun et al, 2005)), *GCNT2* (a glucosaminyl transferase whose recessive mutation causes cataract (Yu et al, 2001)), and *PROX1* (previously mentioned transcription factor, whose mutant causes elongation defects in fiber cells (Wigle et al, 1999). SRA01/04 also expresses decreased levels of *ADAMTSL4* (a transcription factor whose mutation causes ectopia lentis and cataract (Ahram et al, 2009), *SOX2* (a transcription factor whose mutation causes anophthalmia (absence of eyes) (Fantes et al, 2003)), and *STRA6* (a transmembrane receptor for retinoic acid whose mutation also causes anophthalmia (Pasutto et al, 2007) compared to both 21EM15 and HLE-B3. Interestingly, none of the three LEC lines highly express *FOXE3*, a lens epithelial-specific transcription factor whose mutation causes congenital cataract and aniridia (absence of irises) (Bremond-Gignac et al, 2010).

3.3 RT-PCR Validates Human LECs Expression of Key Lens Enriched Genes

From the microarray data, Catmap, and literature searches, 28 candidate genes were chosen to be validated through RT-PCR in both cell lines (Figure 3.3.1). Of these 28 genes, 6 were RNA granule genes, known to code for proteins that were constituents of Stress Granules, Processing Bodies, or both (Figure 3.3.1B). Among the rest of the genes chosen for assay by RT-PCR were crystallin genes (*CRYAB, CRYGS, CRYBB1, CRYGA*), transcription factors (*PROX1, MEIS1, MEIS2, MAFG, PAX6, SOX2*), and structural proteins (*GJA1, CADH1, MIP, VIM*). Furthermore, deficits in *GJA1, MEIS1, JAG1, MAFG, CELF1, TDRD7, PROX1, PAX6, CRYAB, CRYGS, EPHA2,* and *VIM* have all been linked to lens defect or cataracts (Terrell et al, 2015). This RT-PCR data validates the microarray data, showing that HLE-B3 and

SRA01/04 express genes important to lens function and study for the molecular basis of cataract.

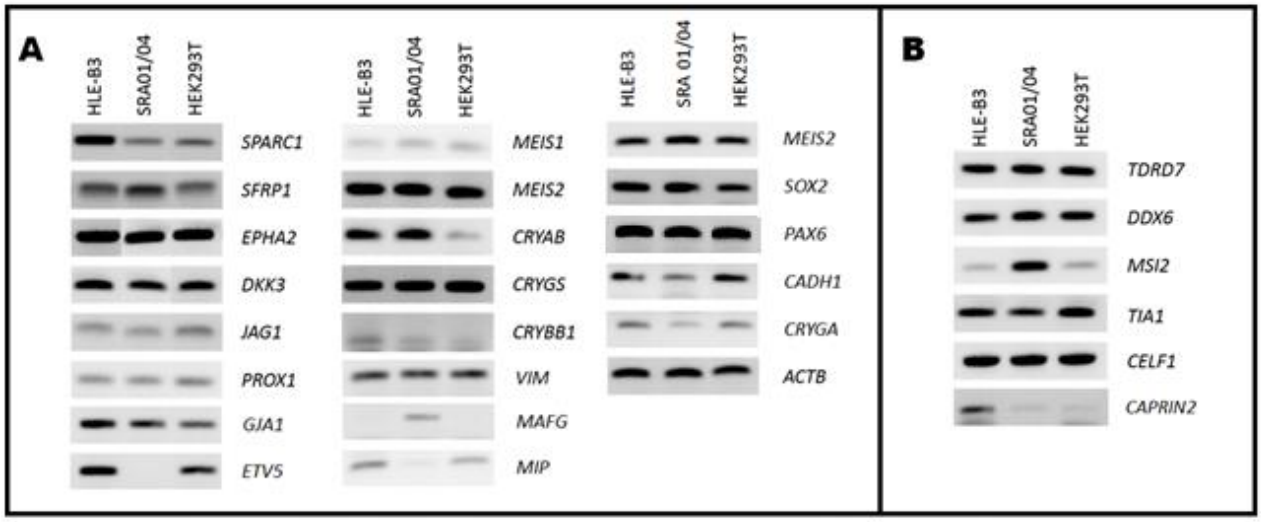

Figure 3.3.1: Investigation of select lens-expressed genes in human lens epithelial cell lines. RT-PCR of validates microarray gene expression of A) important genes for lens function B) RNA granule proteins

3.4 Chemical Stress Significantly Induces Stress Granules and Processing Bodies in Human LECs

In order for the human LEC lines to be appropriate models of lens biology, both lines needed to express constitutive PBs, and SGs under stress conditions. Sodium arsenite has been used to chemically stress cells and induce stress granules both *in vivo* and *in vitro*, and thus was used in this experiment as the first, most robust method of inducing these stresses (McEwen et al, 2005; Kedersha et al, 2002). Previous research has elucidated the role of eIF3b, an early initiation factor, as an

invaluable constituent of SGs, and was therefore used to detect SG formation (Kedersha et al, 2005; Terrell et al, 2015). Ddx6, a DEAD-box RNA helicase, has likewise been evidenced as integral to PB-localized mRNA degradation, and was therefore chosen as a PB marker (Kedersha et al, 2007; Terrell et al, 2015).

After 45 minutes of sodium arsenite stress, both cell lines exhibited significantly increased formation of both PBs and SGs (Figure 3.5.1). Because of the invaluable role of eIF3b in cell translation under normal conditions, unstressed cells still exhibit the protein in high amounts. However, once stressed, the eIF3b complexes into SGs clearly distinguishable as puncta in the high magnification images (and noted by rightward-facing arrowheads). This reaction to oxidative stress through stress granulels is characteristic of previously validated mouse LEC lines under the same chemical stressing conditions (Terrell et al, 2015). PBs also complex en masse when both HLE-B3 and SRA01/04 are chemically stressed, resulting in significantly more PBs than in the unstressed condition in both cell lines (Figure 3.5.2). Additionally, many of the PBs and SGs are co-localized, indicating that the sequestering role of SGs is transitioning into the degrading role of PBs.

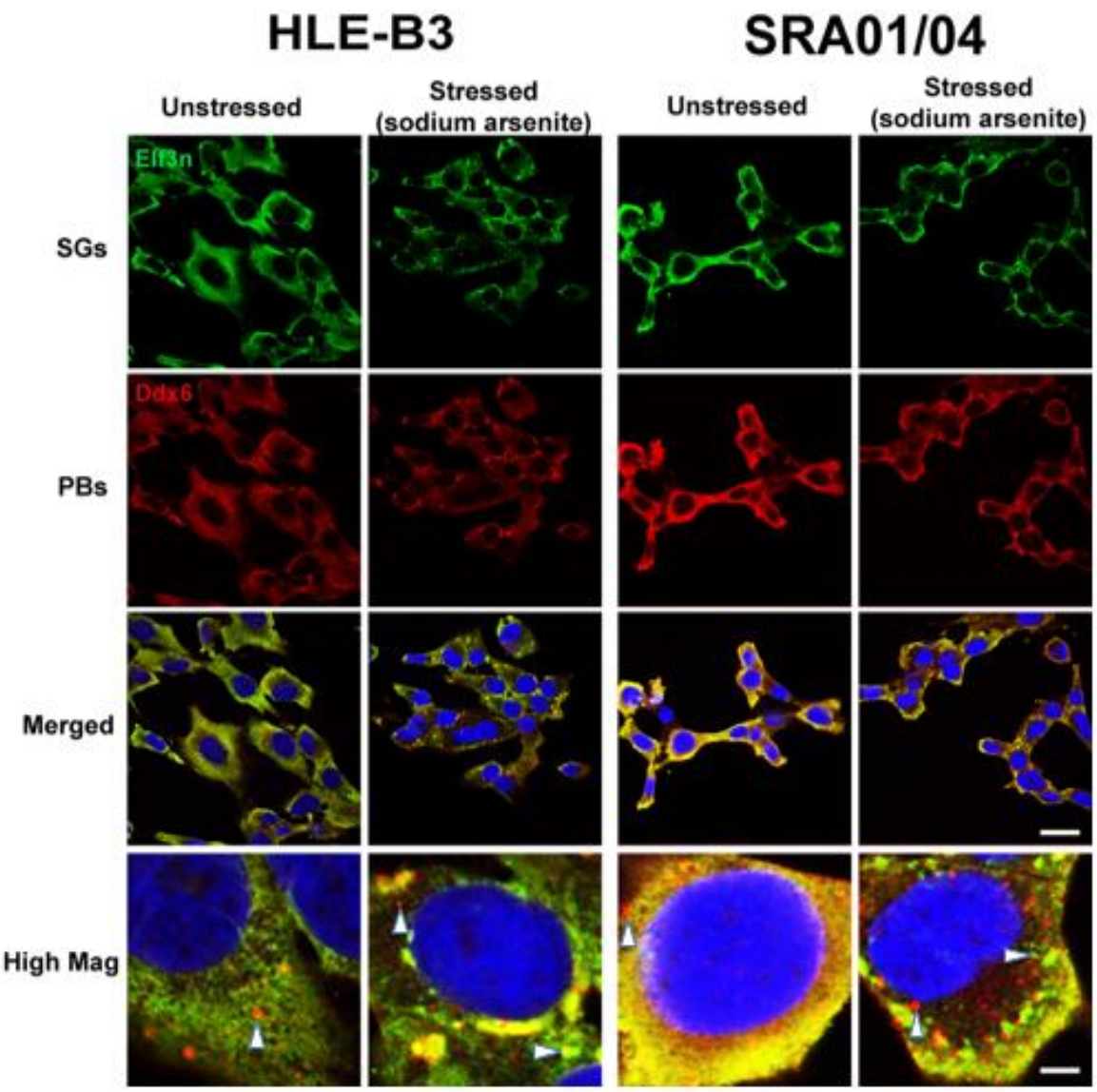

Figure 3.4.1: RNA granule formation in human lens cell lines. Both HLE-B3 and SRA01/04 support formation of Processing Bodies in unstressed conditions and Stress Granules after 45 minutes of sodium arsenite stress. Upward-facing arrowheads denote PBs, and right-facing arrowheads denote SGs

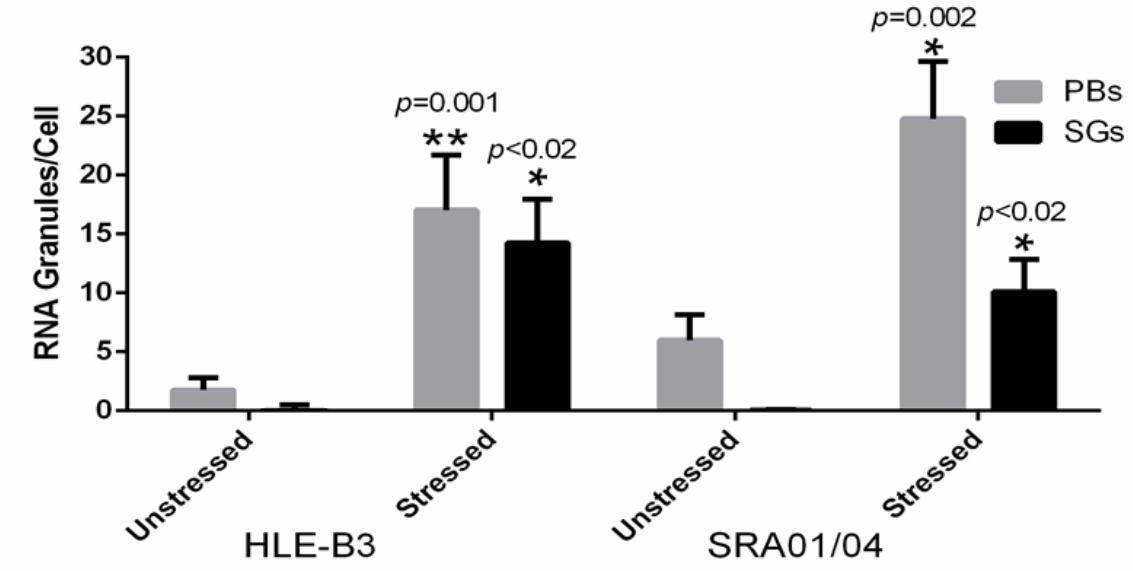

Figure 3.4.2: RNA granules response of human lens cell lines to chemical stress. Both cell lines show significantly upregulated PB and SG formation after chemical stress by sodium arsenite. (N= at least 200 cells)

3.5 UV Stress Significantly Induces Stress Granules and Processing Bodies in Mouse and Human LECs

Though sodium arsenite stress is the standard for inducing stress granules in cells, this study looked to also introduce biologically relevant stressors to the human LEC lines to study their reaction to stress. Thus UV radiation was used to stress both mouse and human LEC lines.

In order to assess RNA Granule formation in a dose-dependent manner, the mouse LEC line 21EM15 was stressed with increasing amounts of UV stress at 15 minute intervals. At 45 minutes of UVA stress, eIF3b can clearly be seen to form distinct puncta, indicating fully complexed stress granules (Figure 3.6.1). At 15 and 30 minutes eIF3b can be seen aggregating, not yet granular, but becoming increasingly concentrated within the cells. This dose-dependent response is interesting not only

from a UV stress point of view, but also for gaining insights on the dynamics of forming SGs.

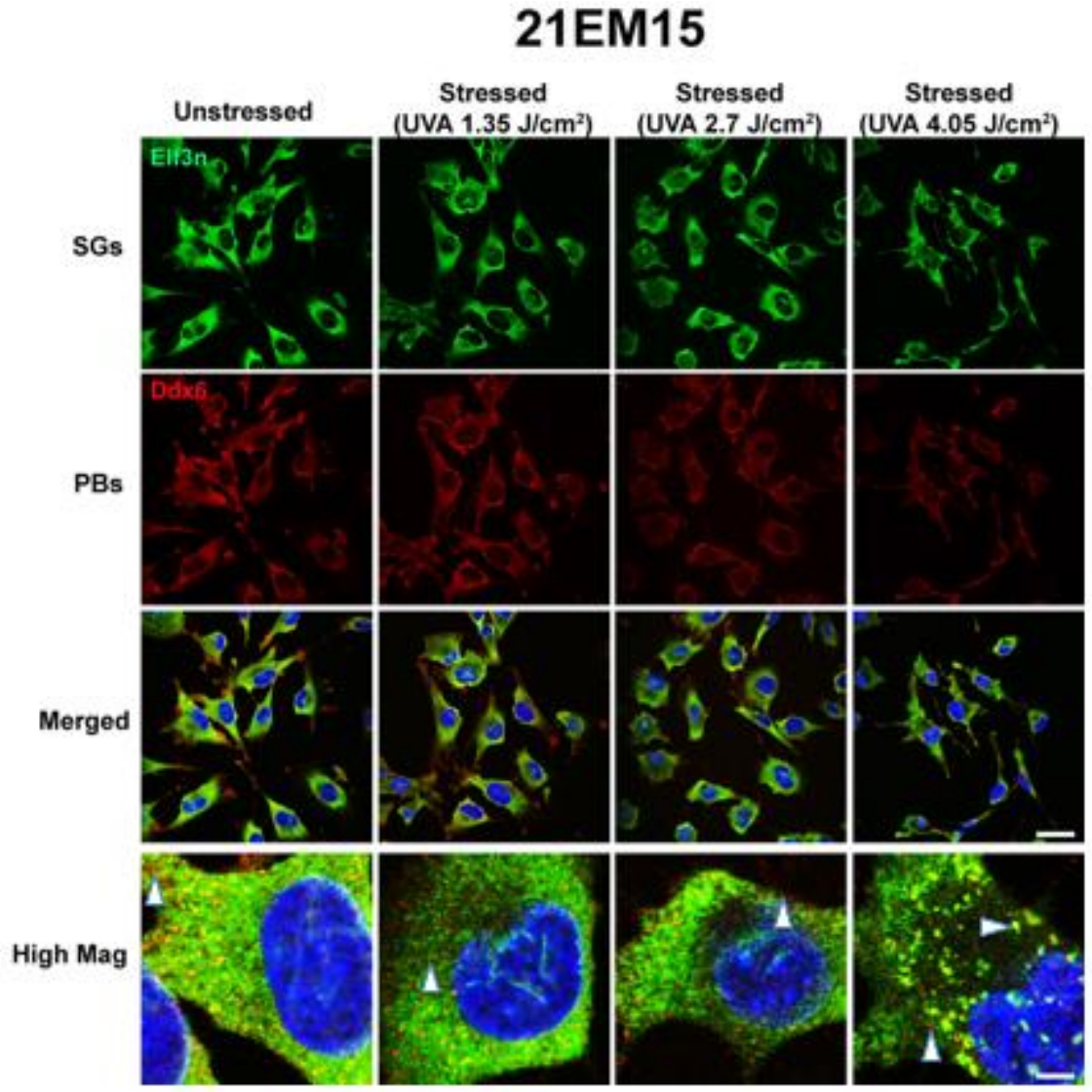

Figure 3.5.1: UV-induced RNA granules in mouse lens epithelial cell line 21EM15. The mouse LEC line 21EM15 supports UV-radiation induced stress granules in a dose-dependent manner. Upward-facing arrowheads denote PBs, and right-facing arrowheads denote SGs (1.35 J/cm^2 = 15 min UVA, 2.7 J/cm^2 = 30 min UVA, 4.05 J/cm^2 = 45 min UVA)

Experiments of dose-dependent UVA-stress on 21EM15 established that LEC lines do respond to UVA stress with RNA granules. With this knowledge, this study moved on to SRA01/04 to study RNA granule reaction to UV stress in a human model of the lens. SRA01/04 reacted even more rapidly to UV stress than 21EM15, forming distinct SGs after only 15 minutes of UVA irradiation (Figure 3.6.2). Formation of SGs and PBs increased dramatically in SRA01/04 after 30 minutes and 60 minutes of UVA irradiation, significantly more than both the unstressed and 15 minute condition (Figure 3.6.3). As in the sodium arsenite stress, the SGs and PBs co-localized to a high degree, especially in the 60 minute stress condition (indicated by yellow granules). Pure bright green SGs are almost absent in the 60 minute UV stress condition, indicating that nearly every SG in that condition is either co-localized with a PB or transitioning into PB-like function (indicated by recruitment of Ddx6).

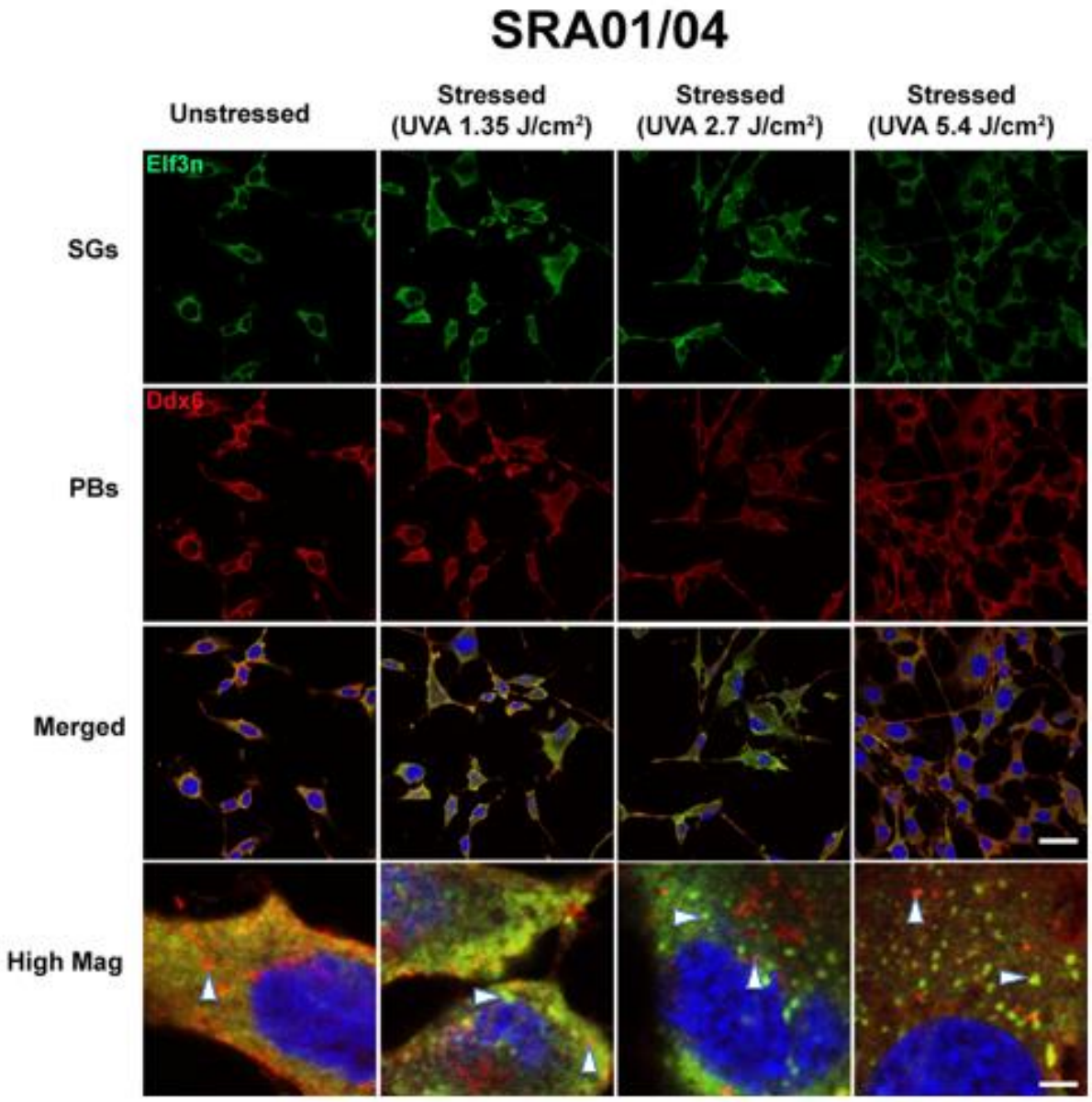

Figure 3.5.2: Dosage effect of UV-induced stress on 21EM15 cells. The mouse LEC line 21EM15 supports UV-radiation induced stress granules in a dose-dependent manner. Upward-facing arrowheads denote PBs, and right-facing arrowheads denote SGs (1.35 J/cm^2 = 15 min UVA, 2.7 J/cm^2 = 30 min UVA, 5.4 J/cm^2 = 60 min UVA)

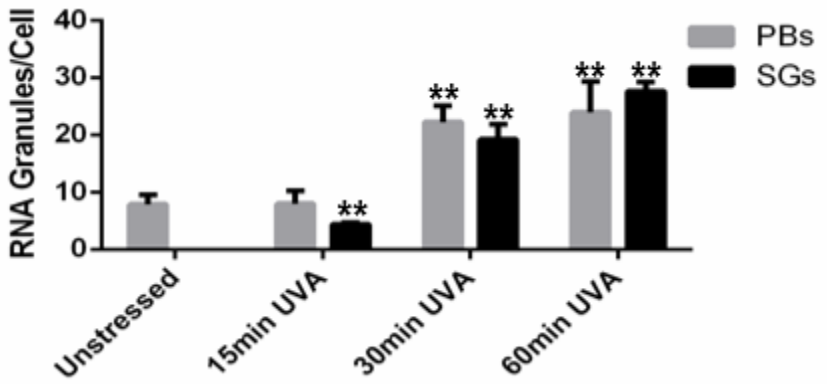

Figure 3.5.3 Response of human lens epithelial cell lines to UV stress. SG and PB formation is significantly upregulated in UV irradiated SRA01/04 cells. (N= greater than 50 cells)

In order to study the RNA granule dynamics of the lens in recovery from UV radiation, SRA01/04 was stressed with 6 J/cm^2 of UVA and allowed to recover before fixation and immunostaining. Slides were allowed to recover for either 30 minutes, 60 minutes, 90 minutes, and 120 minutes in culture media before fixation and staining (3.6.4). After only 30 minutes of recovery, cells show a marked decrease in SGs compared to cells fixed immediately after irradiation. Additionally, the cells given 30 minutes of recovery also appear flatter and to adhere more to the coverslip as opposed to the thin, loosely bound morphology of the cells given no recovery time. Cells allowed an hour of recovery time in media exhibit even less stress granules, and are actively growing outwards, as referenced by various lamellipodia projecting from the recovering cells. After 90 minutes of recovery the cells appear to be almost fully recovered, with only sparse stress granules populating the lamellipodia of the last outgrowing cells. When the cells were allowed 2 hours to recover, they are completely

free of stress granules, and from both a morphological and RNA-granular standpoint appear identical to SRA01/04 cells that were not stressed.

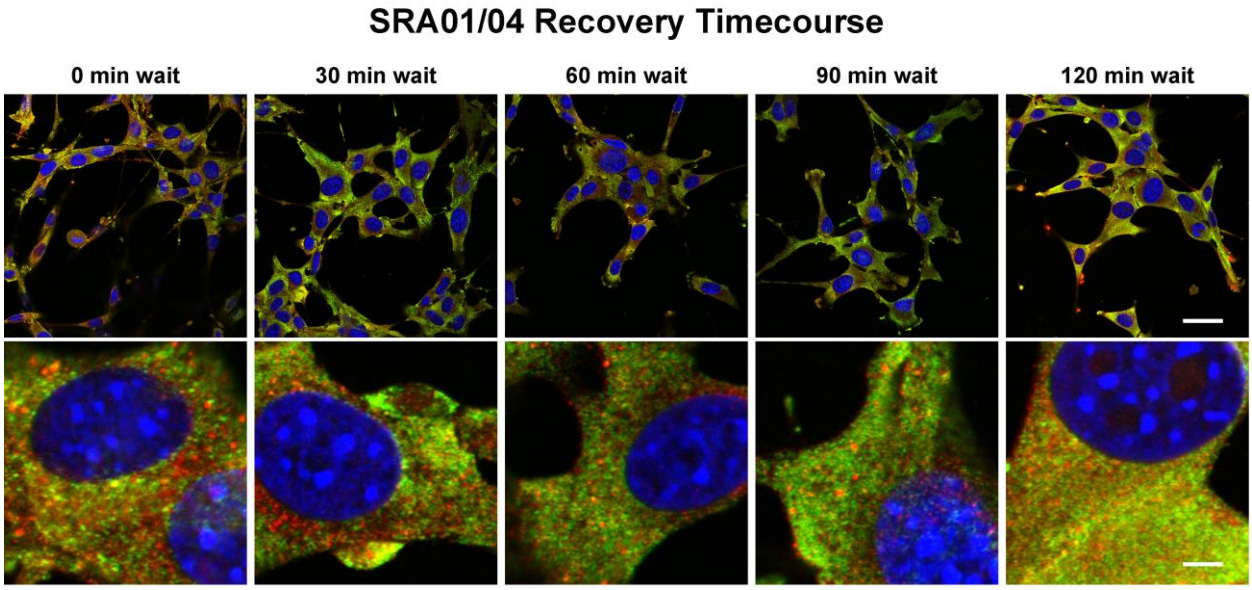

Figure 3.5.4: Recovery time-course of SRA01/04 after UV stress. SRA01/04 after 6 J/cm^2 of UVA stress, fixed and stained after 0 min, 30 min, 60 mins, 90 mins, and 120 mins. (Green: eIF3b 1:300 (SGs), Red: Ddx6 1:300 (PBs), Blue: Draq5 1:2000 (Nuclei))

Chapter 4

DISCUSSION

In vitro tissue models, like cell lines, provide researchers invaluable insights on cellular processes at the molecular level. Cell lines are inexpensive, easily implemented, widely available, highly specific, and self-regenerative, serving as standardized tissue for clear, repeatable results. Despite these advantages, cell lines have come under scrutiny in recent years in light of recent studies elucidating the cross-contamination and misidentification of several widely-used cell lines (American Type Culture Collection Standards Development Organization Workgroup, 2010). Past mishandling of cell lines has called into question the entire practice of using cell lines for biomedical research, and incited the necessity for each cell line to be thoroughly re-evaluated for species of origin and expression of genes characteristic to the cell line's tissue. As of 2014, the American Type Culture Collection (the largest repository of cell lines in the world) has discontinued the sale of 29 cell lines after STR analysis (ATCC, 2016). In order to both uphold past studies that used cell lines and to lend impetus to new studies to use cell lines, emphasis must be placed on international authentication and validation of these important tools.

HLE-B3 and SRA01/04 are two human lens epithelial cell lines that have been used for over 20 years in lens research. This study aimed to: 1) authenticate that both cell lines came from human sources, 2) validate that both cell lines expressed genes that are known to be expressed in the lens *in vivo*, and 3) investigate both cell lines regarding their suitability for RNA granule research. STR analysis of both HLE-B3

and SRA01/04 showed that both these human LEC lines are not only human in origin, but also uniquely human, as they showed no markers for cross-contamination with mouse cell lines. This STR analysis was more comprehensive than the STR analysis used by the ATCC, as HLE-B3 and SRA01/04 were tested with all 13 human CODIS primers, as opposed to the eight used by the ATCC (Reid, 2004). This data unequivocally shows that these human LEC lines can be used as human cell lines in future experiments and lends strong evidence that past studies used human cell lines as well. These cell lines were only screened for contamination with mouse cell lines, and therefore still have the possibility of being cross-contaminated with another species whose primers were not tested (e.g. rat or guinea pig).

The high-throughput, transcriptome-wide assay of both human LEC lines indicates that the cell lines significantly express genes important to lens function and development. Low-throughput RT-PCR assays for important lens-enriched genes upheld the findings of the transcriptome-wide assay, doubly validating that the human LEC lines are lens-like in character. While holistically the human LEC lines have similar expression profiles to both *in vivo* lenses and previously validated *in vitro* LEC lines, certain lens-enriched genes were minimally expressed. Many of these genes are essential for eye development and have been implicated in cataractogenesis, and their diminished presence in the lens could be detrimental to the lens-like nature of the human LEC lines.

Of particular note is the low expression of *ALDH1A1* (an aldehyde dehydrogenase) in both HLE-B3 and SRA01/04 in comparison to 21EM15, because of its role in the lens's response to oxidative stress. The deficiency of *ALDH1A1* has been linked to cataract in rats, mice, and humans, and the opacification is suspected to be

related to the lens's increased susceptibility to oxidative stress (Choudhary, 2005). Both sodium arsenite and UV radiation induce oxidative stress, and the relative lack of *ALDH1A1* could be related to the strong SG reaction of the human LEC lines to these oxidative stressors as a compensation for the lack of *ALDH1A1* contribution. SRA01/04's sensitivity to UV stress supports this idea, as SRA01/04 reacts with SGs after only 1.35 J/cm^2 of UVA stress, while distinct SGs are not seen in 21EM15 until 4.05 J/cm^2 of UVA stress. 21EM15 could be relying on *ALD1H1A1*'s dehydrogenase activity to combat the oxidative stress of UVA at low exposure levels, a pathway SRA01/04 cannot rely on, and thus must recruit SGs much earlier.

Another note in the gene expression of the human LEC lines is the low presence of *CRYGS* in both HLE-B3 and SRA01/04 the microarray data, but the robust expression shown in the RT-PCR. This difference in measured expression can most likely be attributed to an imperfect *CRYGS* probe on the microarray chip underreporting the true level of *CRYGS* transcript present. Indeed, another such example has been observed on the Illumina WG-6 mouse microarrays, on which the Foxe3 probe is not optimal for accurately informing on the expression of this gene (Lachke, unpublished observations).

As evidenced by the RT-PCR data, the qRT-PCR data attempting to assay the differential expression of important lens-enriched genes between HEK293T and the human LEC lines has been inconclusive. Both low-throughput assays of gene expression have shown similar, if not more robust expression of lens-enriched genes in HEK293T compared to SRA01/04. While many lens-enriched genes are also present throughout the body (including the kidney), this data would imply either lower overall gene expression in the human LEC lines, or that HEK293T also has enriched levels of

lens specific genes. In some cases, the high level of expression in HEK293T cells is not surprising, as some of the genes are markers of epithelial cells (e.g. *CADH1* and *GJA1*), and HEK293 is an epithelial cell line. However, for structural crystallins and several transcription factors enriched primarily in the lens, these results are cause for concern whether the human LEC lines are the best cell lines to be modelling lens biology. As stated, this data is not conclusive and is being repeated with new RNA from all cell lines in order to more reliably determine the presence of transcripts in the cell lines.

The induction of SGs through UVA in 21EM15 and SRA01/04 marks the first time SG formation has been observed in the presence of UVA. These data are an exciting new development and open up questions to be answered about not only the methods the lens uses to responds to stress, but the way all mammalian somatic cells respond to stressors. As the lowest frequency and longest wavelength of UV radiation, the detrimental effects UVA can inflict on cells is often overlooked in favor of the much faster acting, higher energy UVB and UVC. However, these experiments demonstrate that UVA induces a stress response on the magnitude of sodium arsenite after only 15 minutes of irradiation in SRA01/04. This is particularly relevant considering that nearly 97% of the UV light in the atmosphere is UVA, and from that up to 80% of UVA passes through the cornea and aqueous humor directly to the lens (Hammond et al, 2014). As such, UVA may be the most relevant biological stressor of the lens and especially the lens epithelium at the anterior of the lens (therefore absorbing the brunt of the UVA). This data indicates that SGs may be one of the primary responses of LECs to UVA, and as such are invaluable to the maintenance of a healthy lens. The specific proteins recruited in SGs responding to UVA stress, as

well as the amount of oxidative stress (measured by GSH) caused by UVA stress both for the formation of SGs and without the function of SGs are key experiments in the future for determining the molecular basis for age-related cataracts. An immediate future direction of this study will compare the effect of UVB and UVA on SG formation in the human LEC lines.

The increased levels of stress granules and processing bodies in the lamellipodia of recovering cells could indicate that after stress, outgrowth is prioritized over the dissociation of stress granules. Another explanation could be that stress granules are involved in the relocalization of mRNA during LEC recovery after intense UV stress. While RNA granules are commonly found within lamellipodia as a means of mRNA localization (Shav-Tal & Singer, 2005), stress granules have yet to be implicated in this process. Another explanation for the high levels of eIF3b in the lamellipodia (especially at the leading edge) could be that the cytoplasm squeezed into the small pockets of the distal lamellipodia is more concentrated (thus the "granules" are artifacts of closely-spaced but not complexed eIF3b), or these stress granules have yet to receive signals from the cell body instructing them to disassemble. Whatever the explanation for stress granule localization in the lamellipodia, it can be seen throughout the UV recovery process of SRA01/04. Additional experiments closely examining the dynamics of SG disassembly after UV stress and sodium arsenite stress can further elucidate which transcripts the cell prioritizes after recovery from stress. This could be examined by comparing protein expression during stress to protein expression at time points after stressing to determine which transcripts are most readily re-initiated as the cell returns to homeostasis.

In vivo experiments to determine the formation of SGs in mouse lenses have so far been inconclusive. Experiments to induce and assay SG formation in the lenses of whole eyes irradiated with varying levels of UVA and UVB are ongoing. These data would not only serve to show SGs as a response to UV radiation in the context of a more complete organ, but would also further validate the use of HLE-B3 and SRA01/04 as tools to gain insight on the mechanisms in play within *in vivo* lenses. Additionally antibodies against Dcp1a, TIA-1, and TIAR have been used in attempts to assay SG response to UV stress in mice in addition to the Ddx6 and eIF3b antibodies that formed RGs in the human LEC lines. These methods have not yet yielded results, but iterations of stress and assays of SGs have not yet been exhausted.

This study has authenticated the human LEC lines HLE-B3 and SRA01/04 as human lens cells, and validated that both cell lines express many genes expressed or enriched in the lens *in vivo*. Additionally, both cell lines support the formation of PBs under unstressed conditions and the formation of SGs and increase in PBs under both chemical and UV stress. These data together indicate that HLE-B3 and SRA01/04 are appropriate models of lens biology and can be used for further study on cataract-associated genes. The induction of SGs through UVA in SRA01/04 and the mouse cell line 21EM15 opens up a new perspective on how the lens responds to relevant stressors, and hopefully will lead to further progress on the prevention and treatment of age-related cataract.

REFERENCES

If you want to number your bibliographic entries, change the style of the items to *Bib Entry - numbered*.

Azari, S., Ahmadi, N., Tehrani, M. J., & Shokri, F. (2007). Profiling and authentication of human cell lines using short tandem repeat (STR) loci: Report from the National Cell Bank of Iran. Biologicals,35(3), 195-202.

Chambers GK, MacAvoy ES. Microsatellites: consensus and controversy. Comp Biochem Physiol B 2000;126:455e76.

Miller KWP, Brown BL, Budowle B. The Combined DNA Index System. Int Congr Ser 2003;1239:617e20.

Masters JR, Thomson JA, Daly-Burns B, Reid YA, Dirks WG, Packer P, et al. Short tandem repeat profiling provides an international reference standard for human cell lines. Proc Natl Acad Sci U S A 2001;98:8012e7.

Masibay A, Mozer TJ, Sprecher C. Promega Corporation reveals primer sequences in its testing kits. J Forensic Sci 2000;45:1360e2.

Ruitberg CM, Reeder DJ, Butler JM. STRBase: a short tandem repeat DNA database for the human identity testing community. Nucleic Acids Res 2001;29:320e2.

Almeida, J. L., Hill, C. R., & Cole, K. D. (2014). Mouse cell line authentication. Cytotechnology,66(1), 133-147.

Butler, J.M. (2006) Genetics and genomics of core STR loci used in human identity testing. J. Forensic Sci. 51(2): 253-265.

McEwen, E., Kedersha, N., Song, B., Scheuner, D., Gilks, N., Han, A., ... & Kaufman, R. J. (2005). Heme-regulated inhibitor kinase-mediated phosphorylation of eukaryotic translation initiation factor 2 inhibits translation, induces stress granule formation, and mediates survival upon arsenite exposure. Journal of Biological Chemistry,280(17), 16925-16933.

Arimoto, K., Fukuda, H., Imajoh-Ohmi, S., Saito, H., & Takekawa, M. (2008). Formation of stress granules inhibits apoptosis by suppressing stress-responsive MAPK pathways. Nature cell biology,10(11), 1324-1332.

Kedersha, Nancy, Samantha Chen, Natalie Gilks, Wei Li, Ira J. Miller, Joachim Stahl, and Paul Anderson. "Evidence that ternary complex (eIF2-GTP-tRNAi Met)–deficient preinitiation complexes are core constituents of mammalian stress granules." Molecular biology of the cell 13, no. 1 (2002): 195-210.

Kedersha, N., & Anderson, P. (2007). Mammalian stress granules and processing bodies. Methods in enzymology, 431, 61-81.

Kedersha, N., Stoecklin, G., Ayodele, M., Yacono, P., Lykke-Andersen, J., Fritzler, M. J., ... & Anderson, P. (2005). Stress granules and processing bodies are dynamically linked sites of mRNP remodeling. The Journal of cell biology,169(6), 871-884.

Wang, Y., Arribas-Layton, M., Chen, Y., Lykke-Andersen, J., & Sen, G. L. (2015). DDX6 Orchestrates Mammalian Progenitor Function through the mRNA Degradation and Translation Pathways. Molecular cell, 60(1), 118-130.

Pothof, J., Verkaik, N. S., van IJcken, W., Wiemer, E. A., Ta, V. T., van der Horst, G. T., ... & Persengiev, S. P. (2009). MicroRNA-mediated gene silencing modulates the UV-induced DNA-damage response. The EMBO journal, 28(14), 2090-2099.

Tan, G., Shi, Y., & Wu, Z. H. (2012). MicroRNA-22 promotes cell survival upon UV radiation by repressing PTEN. Biochemical and biophysical research communications, 417(1), 546-551.

Midelfart, A. (2005). Ultraviolet radiation and cataract. Acta Ophthalmologica Scandinavica,83(6), 642-644.

Taylor, H. R., West, S. K., Rosenthal, F. S., Muñoz, B., Newland, H. S., Abbey, H., & Emmett, E. A. (1988). Effect of ultraviolet radiation on cataract formation. New England Journal of Medicine,319(22), 1429-1433.

Moutaoufik, M. T., El Fatimy, R., Nassour, H., Gareau, C., Lang, J., Tanguay, R. M., ... & Khandjian, E. W. (2014). UVC-induced stress granules in mammalian cells. PloS one, 9(11), e112742.

Dolin, P. J. (1994). Ultraviolet radiation and cataract: a review of the epidemiological evidence.The British journal of ophthalmology, 78(6), 478.

Kakar, M. K., Mody Jr, V. C., Löfgren, S., Ayala, M., Dong, X., & Söderberg, P. G. (2004). Evolution of Ultraviolet Radiation–B (UVR–B)–Induced Cataract in the Pigmented Guinea Pig. Investigative Ophthalmology & Visual Science, 45(13), 385-385.

Zhang, J., Yan, H., Löfgren, S., Tian, X., & Lou, M. F. (2012). Ultraviolet Radiation–Induced Cataract in Mice: The Effect of Age and the Potential Biochemical MechanismBiochemical Mechanism of UV-Induced Damage in the Lens. Investigative ophthalmology & visual science, 53(11), 7276-7285.

Ayala, M. N., Michael, R., & Söderberg, P. G. (2000). Influence of exposure time for UV radiation–induced cataract. Investigative ophthalmology & visual science, 41(11), 3539-3543.

Malina, H. Z., & Martin, X. D. (1995). Deamination of 3-hydroxykynurenine in bovine lenses: a possible mechanism of cataract formation in general. Graefe's archive for clinical and experimental ophthalmology, 233(1), 38-44.

Roberts, J. E. (2011). Photobiology of the Human Lens. Original research article, Fordham University, Department of Natural Sciences, New York, NY.

Barker, FM, Brainard GC and Dayhaw-Barker P (1991) Transmittance of the human lens as a function of age. Invest. Ophthalmol. Vis. Sci. 32S p. 1083.

Roberts JE. (2001) Ocular phototoxicity. J. Photochem. Photobiol. B: Biology 64, 136-143.

Minassian, D. C., & Mehra, V. (1990). 3.8 million blinded by cataract each year: projections from the first epidemiological study of incidence of cataract blindness in India. British journal of ophthalmology,74(6), 341-343.

Hammond, B. R., Johnson, B. A., & George, E. R. (2014). Oxidative photodegradation of ocular tissues: beneficial effects of filtering and exogenous antioxidants. Experimental eye research, 129, 135-150.

Beyer, E. C., & Berthoud, V. M. (2015). Connexin hemichannels in the lens. Hemichannels; from the molecule to the function, 52.

Xi, J., Bai, F., Patel, H. C., & Andley, U. P. (2003). Identification of Genes Responsive to UVA Radiation in Human Lens Epithelial Cells using cDNA Microarrays. Investigative Ophthalmology & Visual Science, 44(13), 302-302.

Heo, J., Lee, B. R., & Koh, J. W. (2008). Protective effects of epigallocatechin gallate after UV irradiation of cultured human lens epithelial cells.Korean Journal of Ophthalmology, 22(3), 183-186.

Shin, D. M., Jeon, J. H., Kim, C. W., Cho, S. Y., Kwon, J. C., Lee, H. J., ... & Kim, I. G. (2004). Cell Type-specific Activation of Intracellular Transglutaminase 2 by Oxidative Stress or Ultraviolet Irradiation IMPLICATIONS OF TRANSGLUTAMINASE 2 IN AGE-RELATED CATARACTOGENESIS. Journal of Biological Chemistry, 279(15), 15032-15039.

Obrenovich, M. E., Fan, X., Satake, M., Jarvis, S. M., Reneker, L., Reddan, J. R., & Monnier, V. M. (2006). Relative suppression of the sodium-dependent Vitamin C transport in mouse versus human lens epithelial cells. Molecular and cellular biochemistry, 293(1-2), 53-62.

Andley, U. P., Becker, B., Hebert, J. S., Reddan, J. R., Morrison, A. R., & Pentland, A. P. (1996). Enhanced prostaglandin synthesis after ultraviolet-B exposure modulates DNA synthesis of lens epithelial cells and lowers intraocular pressure in vivo. Investigative ophthalmology & visual science,37(1), 142-153.

Osada, H., Yoshitake, Y., Ikeda, T., Ishigaki, Y., Takata, T., Tomosugi, & Yonekura, H. (2011). Ultraviolet B-induced expression of amphiregulin and growth differentiation factor 15 in human lens epithelial cells.

Yao, K., Zhang, L., Zhang, Y., Ye, P., & Zhu, N. (2008). The flavonoid, fisetin, inhibits UV radiation-induced oxidative stress and the activation of NF-κB and MAPK signaling in human lens epithelial cells.

Okuno, T. (2007). Ultraviolet action spectrum for cell killing in a human lens epithelial cell line.Industrial health, 45(1), 137-142.

Sachdev, N. H., Di Girolamo, N., Nolan, T. M., McCluskey, P. J., Wakefield, D., & Coroneo, M. T. (2004). Matrix metalloproteinases and tissue inhibitors of matrix metalloproteinases in the human lens: implications for cortical cataract formation. Investigative ophthalmology & visual science, 45(11), 4075-4082.

Shui, Y. B., Sasaki, H., Pan, J. H., Hata, I., Kojima, M., Yamada, Y. & Sasaki, K. (2000). Morphological observation on cell death and phagocytosis induced by ultraviolet irradiation in a cultured human lens epithelial cell line.Experimental eye research, 71(6), 609-618.

Kaur, G., & Dufour, J. M. (2012). Cell lines: Valuable tools or useless artifacts. Spermatogenesis, 2(1), 1-5.

ATCC. (2016). Cell Lines. Retrieved April 13, 2016, from http://www.atcc.org/Products/Cells and Microorganisms/Cell Lines.aspx

ATCC. (2016). Misidentified Cell Lines. Retrieved April 13, 2016, from http://www.atcc.org/Products/Cells and Microorganisms/Cell Lines/ Misidentified_Cell_Lines.aspx

NEI. (2016). Cataract. Retrieved March 14, 2016, from https://nei.nih.gov/health/cataract/.

NEI. (2016). Cataract Data and Statistics. Retrieved March 14, 2016, from https://nei.nih.gov/eyedata/cataract/.

Wilmer Eye Institute. (2016). Retrieved March 14, 201, from http://www.hopkinsmedicine.org/wilmer/conditions/cataracts_faq.html

Wang-Su, S. T., McCormack, A. L., Yang, S., Hosler, M. R., Mixon, A., Riviere, M. A., ... & David, L. L. (2003). Proteome analysis of lens epithelia, fibers, and the HLE B-3 cell line. Investigative ophthalmology & visual science, 44(11), 4829-4836.

Beebe, D.C., 2013. The use of cell lines to "model" ocular tissues: cautionary tales. Invest. Ophthalmol. Vis. Sci. 54 http://dx.doi.org/10.1167/iovs.13-12873.

The Editors of Molecular Vision, 2013. On authentication of cell lines. Molecular Vision 2013: 19:1848-51

The Editors of Experimental Eye Research, 2013. On the use of immortalized ocular cell lines in vision research: The unfortunate story of RGC-5. Experimental Eye Research 116:433

Krishnamoorthy, R. R., Clark, A. F., Daudt, D., Vishwanatha, J. K., & Yorio, T. (2013). A Forensic Path to RGC-5 Cell Line Identification: Lessons LearnedMisidentification of RGC-5 Cells.Investigative ophthalmology & visual science,54(8), 5712-5719.

Zampighi, G. A., Eskandari, S., & Kreman, M. (2000). Epithelial organization of the mammalian lens. Experimental eye research, 71(4), 415-435.

Cogan, D. G. (1962). Anatomy of lens and pathology of cataracts. Experimental eye research,1(4), 291-IN3.

Toates, F. M. (1972). Accommodation function of the human eye. Physiological Reviews, 52(4), 828-863.

McAvoy, J. W., Chamberlain, C. G., de Longh, R. U., Hales, A. M., & Lovicu, F. J. (1999). Lens development. Eye, 13, 425-437.

Lovicu FJ, McAvoy JW. Structural analysis of lens epithelial explants induced to differentiate into fibres by fibroblast growth factor (FGF). Exp Eye Res 1989;49:479-94.

Chamberlain CG, McAvoy JW. Fibre differentiation and polarity in the mammalian lens: a key role for FGF. Prog Ret Eye Res 1997;16:443-78.

Blakely, E. A., K. A. Bjornstad, P. Y. Chang, M. P. McNamara, E. Chang, G. Aragon, S. P. Lin, G. Lui, and J. R. Polansky, 2000, Growth and differentiation of human lens epithelial cells in vitro on matrix: Invest Ophthalmol Vis Sci, v. 41, p. 3898-907.

Cvekl, A., and M. K. Duncan, 2007, Genetic and epigenetic mechanisms of gene regulation during lens development: Prog Retin Eye Res, v. 26, p. 555-97.

Kumar, P. A., & Reddy, G. B. (2009). Modulation of α-crystallin chaperone activity: A target to prevent or delay cataract?. IUBMB life, 61(5), 485-495.

Lachke, S. A., & Maas, R. L. (2011). RNA granules and cataract. Expert review of ophthalmology, 6(5), 497-500.

Foster, A., & Resnikoff, S. (2005). The impact of Vision 2020 on global blindness. Eye, 19(10), 1133-1135.

Ogino, H., Ochi, H., Reza, H. M., & Yasuda, K. (2012). Transcription factors involved in lens development from the preplacodal ectoderm. *Developmental biology*, *363*(2), 333-347.Shav-Tal, Y., & Singer, R. H. (2005). RNA localization. Journal of Cell Science, 118(18), 4077-4081.

Hayashi, R., Ishikawa, Y., Sasamoto, Y., Katori, R., Nomura, N., Ichikawa & Quantock, A. J. (2016). Co-ordinated ocular development from human iPS cells and recovery of corneal function.Nature, 531(7594), 376-380.

Zhao, L., Chen, X. J., Zhu, J., Xi, Y. B., Yang, X., Hu, L. D., ... & Wu, F. (2015). Lanosterol reverses protein aggregation in cataracts. Nature.

Brown, G. C., M. M. Brown, A. Menezes, B. G. Busbee, H. B. Lieske, and P. A. Lieske, 2013, Cataract Surgery Cost Utility Revisited in 2012 : A New Economic Paradigm: Ophthalmology, v. 120, p. 2367–2376.

Lovicu, F. J., and M. L. Robinson, 2004, Development of the Ocular Lens, Cambridge University Press.

Michael, R., and A. J. Bron, 2011, The ageing lens and cataract: a model of normal and pathological ageing: Philos Trans R Soc Lond B Biol Sci, v. 366, p. 1278-92.

Nishimoto, S., K. Kawane, R. Watanabe-Fukunaga, H. Fukuyama, Y. Ohsawa, Y. Uchiyama, N. Hashida, N. Ohguro, Y. Tano, T. Morimoto, Y. Fukuda, and S. Nagata, 2003, Nuclear cataract caused by a lack of DNA degradation in the mouse eye lens: Nature, v. 424, p. 1071-4.

Moreau, K. L. & King, J. A. Protein misfolding and aggregation in cataract disease and prospects for prevention. Trends Mol. Med. 18, 273–282 (2012)

Andley, U. P. (2007). Crystallins in the eye: function and pathology. Progress in retinal and eye research, 26(1), 78-98.

J. Horwitz, M.P. Bova, L.L. Ding, D.A. Haley, P.L. Stewart. Lens alpha-crystallin: function and structure. Eye, 13 (Pt 3b) (1999), pp. 403–408

Benedek, G. B., Pande, J., Thurston, G. M., & Clark, J. I. (1999). Theoretical and experimental basis for the inhibition of cataract. Progress in retinal and eye research, 18(3), 391-402.

Asbell, P. A., I. Dualan, J. Mindel, D. Brocks, M. Ahmad, and S. Epstein, 2005, Age-related cataract: Lancet, v. 365, p. 599-609.

Shiels, A., T. M. Bennett, and J. F. Hejtmancik, 2010, Cat-Map: putting cataract on the map: Mol Vis, v. 16, p. 2007-15.

Anand, D., & Lachke, S. A. (2016). Systems biology of lens development: A paradigm for disease gene discovery in the eye. Experimental Eye Research.

Agrawal, S. A., Anand, D., Siddam, A. D., Kakrana, A., Dash, S., Scheiblin, D. A., ... & Motohashi, H. (2015). Compound mouse mutants of bZIP transcription factors Mafg and Mafk reveal a regulatory network of non-crystallin genes associated with cataract. Human genetics, 134(7), 717-735.

Dash, S., Dang, C. A., Beebe, D. C., & Lachke, S. A. (2015). Deficiency of the RNA binding protein caprin2 causes lens defects and features of peters anomaly. Developmental Dynamics, 244(10), 1313-1327.

Kasaikina, M. V., Fomenko, D. E., Labunskyy, V. M., Lachke, S. A., Qiu, W., Moncaster, J. A., ... & Schweizer, U. (2011). Roles of the 15-kDa selenoprotein (Sep15) in redox homeostasis and cataract development revealed by the analysis of Sep 15 knockout mice. Journal of Biological Chemistry, 286(38), 33203-33212.

Lachke, S. A., Alkuraya, F. S., Kneeland, S. C., Ohn, T., Aboukhalil, A., Howell, G. R., ... & Nair, K. S. (2011). Mutations in the RNA granule component TDRD7 cause cataract and glaucoma.Science, 331(6024), 1571-1576.

Lachke, S. A., Higgins, A. W., Inagaki, M., Saadi, I., Xi, Q., Long, M., ... & Robinson, M. L. (2012). The cell adhesion gene PVRL3 is associated with congenital ocular defects. Human genetics, 131(2), 235-250.

Glisovic, T., Bachorik, J. L., Yong, J., & Dreyfuss, G. (2008). RNA-binding proteins and post-transcriptional gene regulation. FEBS letters,582(14), 1977-1986.

ZIGMAN, S. (1995). Environmental near-UV radiation and cataracts. Optometry & Vision Science, 72(12), 899-901.

Lachke, S. A., & Maas, R. L. (2011). RNA granules and cataract. Expert review of ophthalmology, 6(5), 497-500.

Oleynikov, Y., & Singer, R. H. (2003). Real-time visualization of ZBP1 association with β-actin mRNA during transcription and localization.Current Biology, 13(3), 199-207.

Anderson, P., & Kedersha, N. (2009). RNA granules: post-transcriptional and epigenetic modulators of gene expression. Nature reviews Molecular cell biology, 10(6), 430-436.

Kedersha, N., & Anderson, P. (2007). Mammalian stress granules and processing bodies. Methods in enzymology, 431, 61-81.

Castello, A., Fischer, B., Eichelbaum, K., Horos, R., Beckmann, B. M., Strein, C., ... & Krijgsveld, J. (2012). Insights into RNA biology from an atlas of mammalian mRNA-binding proteins. Cell, 149(6), 1393-1406.

Lukong, K. E., Chang, K. W., Khandjian, E. W., & Richard, S. (2008). RNA-binding proteins in human genetic disease. Trends in Genetics, 24(8), 416-425.

Anderson, P., & Kedersha, N. (2006). RNA granules. The Journal of cell biology, 172(6), 803-808.

Bashkirov, V. I., Scherthan, H., Solinger, J. A., Buerstedde, J. M., & Heyer, W. D. (1997). A mouse cytoplasmic exoribonuclease (mXRN1p) with preference for G4 tetraplex substrates. The Journal of cell biology, 136(4), 761-773.

Gilks, N., Kedersha, N., Ayodele, M., Shen, L., Stoecklin, G., Dember, L. M., & Anderson, P. (2004). Stress granule assembly is mediated by prion-like aggregation of TIA-1. Molecular biology of the cell, 15(12), 5383-5398.

Kedersha, N., Stoecklin, G., Ayodele, M., Yacono, P., Lykke-Andersen, J., Fritzler, M. J., ... & Anderson, P. (2005). Stress granules and processing bodies are dynamically linked sites of mRNP remodeling. The Journal of cell biology,169(6), 871-884.

Nover, L. U. T. Z., Scharf, K. D., & Neumann, D. I. E. T. E. R. (1989). Cytoplasmic heat shock granules are formed from precursor particles and are associated with a specific set of mRNAs.Molecular and Cellular Biology, 9(3), 1298-1308.

Buchan, J. R., & Parker, R. (2009). Eukaryotic stress granules: the ins and outs of translation.Molecular cell, 36(6), 932-941.

Yamashita, A., Chang, T. C., Yamashita, Y., Zhu, W., Zhong, Z., Chen, C. Y. A., & Shyu, A. B. (2005). Concerted action of poly (A) nucleases and decapping enzyme in mammalian mRNA turnover.Nature structural & molecular biology, 12(12), 1054-1063.

Reijns, M. A., Alexander, R. D., Spiller, M. P., & Beggs, J. D. (2008). A role for Q/N-rich aggregation-prone regions in P-body localization.Journal of cell science, 121(15), 2463-2472.

Giménez-Barcons, M., & Díez, J. (2011). Yeast processing bodies and stress granules: self-assembly ribonucleoprotein particles. Microbial cell factories, 10(1), 1.

Kedersha, N., Ivanov, P., & Anderson, P. (2013). Stress granules and cell signaling: more than just a passing phase?. Trends in biochemical sciences,38(10), 494-506.

Ongusaha, P. P., Qi, H. H., Raj, L., Kim, Y. B., Aaronson, S. A., Davis, R. J., ... & Lee, S. W. (2008). Identification of ROCK1 as an upstream activator of the JIP-3 to JNK signaling axis in response to UVB damage. Science signaling,1(47), ra14.

Kedersha, N. L., Gupta, M., Li, W., Miller, I., & Anderson, P. (1999). RNA-binding proteins TIA-1 and TIAR link the phosphorylation of eIF-2α to the assembly of mammalian stress granules. The Journal of cell biology, 147(7), 1431-1442.

Kedersha, N., Ivanov, P., & Anderson, P. (2013). Stress granules and cell signaling: more than just a passing phase?. Trends in biochemical sciences,38(10), 494-506.

Buchan, J. R., Yoon, J. H., & Parker, R. (2011). Stress-specific composition, assembly and kinetics of stress granules in Saccharomyces cerevisiae.Journal of cell science, 124(2), 228-239.

Jivotovskaya, A. V., Valášek, L., Hinnebusch, A. G., & Nielsen, K. H. (2006). Eukaryotic translation initiation factor 3 (eIF3) and eIF2 can promote mRNA binding to 40S subunits independently of eIF4G in yeast. Molecular and Cellular Biology,26(4), 1355-1372.

Choudhary, S., Xiao, T., Vergara, L. A., Srivastava, S., Nees, D., Piatigorsky, J., & Ansari, N. H. (2005). Role of aldehyde dehydrogenase isozymes in the defense of rat lens and human lens epithelial cells against oxidative stress. Investigative ophthalmology & visual science, 46(1), 259-267.

Sun, H., Ma, Z., Li, Y., Liu, B., Li, Z., Ding, X., ... & Shen, Y. (2005). Gamma-S crystallin gene (CRYGS) mutation causes dominant progressive cortical cataract in humans. Journal of medical genetics, 42(9), 706-710.

Yu, L. C., Twu, Y. C., Chang, C. Y., & Lin, M. (2001). Molecular basis of the adult i phenotype and the gene responsible for the expression of the human blood group I antigen. Blood, 98(13), 3840-3845.

Wigle, J. T., & Oliver, G. (1999). Prox1 function is required for the development of the murine lymphatic system. Cell, 98(6), 769-778.

Pasutto, F., Sticht, H., Hammersen, G., Gillessen-Kaesbach, G., FitzPatrick, D. R., Nürnberg, G., ... & Houge, G. (2007). Mutations in STRA6 cause a broad spectrum of malformations including anophthalmia, congenital heart defects, diaphragmatic hernia, alveolar capillary dysplasia, lung hypoplasia, and mental retardation. The American Journal of Human Genetics, 80(3), 550-560.

Ahram, D., Sato, T. S., Kohilan, A., Tayeh, M., Chen, S., Leal, S., ... & El-Shanti, H. (2009). A homozygous mutation in ADAMTSL4 causes autosomal-recessive isolated ectopia lentis. The American Journal of Human Genetics, 84(2), 274-278.

Fantes, J., Ragge, N. K., Lynch, S. A., McGill, N. I., Collin, J. R. O., Howard-Peebles, P. N., ... & FitzPatrick, D. R. (2003). Mutations in SOX2 cause anophthalmia. Nature genetics, 33(4), 462-463.

Brémond-Gignac, D., Bitoun, P., Reis, L. M., Copin, H., Murray, J. C., & Semina, E. V. (2010). Identification of dominant FOXE3 and PAX6 mutations in patients with congenital cataract and aniridia.

American Type Culture Collection Standards Development Organization Workgroup ASN-0002. (2010). Cell line misidentification: the beginning of the end. Nature Reviews Cancer, 10(6).

Reid, Y., Storts, D., Riss, T., & Minor, L. (2004). Authentication of human cell lines by STR DNA profiling analysis.

Appendix A

SUPPLEMENTARY METHODS

Authentication PCR Reaction Mixture:

Reagent	**Volume (µL)**
H_2O	19.
Coral Red Buffer (10X)	2.5
$MgCl_2$	0.75
dNTP	0.5
Forward Primer (10mM)	0.5
Reverse Primer (10mM)	0.5
Taq Polymerase	0.25
gDNA	0.5
Total	**25.00**

RT-PCR Reaction Mixture:

Reagent	**Volume (µL)**
H_2O	20.1
Coral Red Buffer (10X)	2.5
dNTP	0.5
Forward Primer (10mM)	0.5

Reverse Primer (10mM)	0.5
Taq Polymerase	0.25
cDNA	0.65
Total	**25.00**